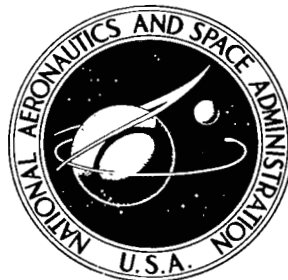


NASA TECHNICAL NOTE



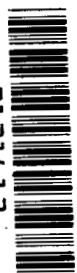
NASA TN D-4855

0.1

NASA TN D-4855

LOAN COPY: RETURN TO
AFWL (WLIL-2)
KIRTLAND AFB, N

0131613



TECH LIBRARY KAFB, NM

AERODYNAMIC CHARACTERISTICS OF A
PARASOL-WING—BODY COMBINATION
UTILIZING FAVORABLE LIFT INTERFERENCE
AT MACH NUMBERS FROM 3.00 TO 4.63

by Odell A. Morris and Robert J. Mack

Langley Research Center

Langley Station, Hampton, Va.



0131613

NASA TN D-4855

✓
AERODYNAMIC CHARACTERISTICS OF A PARASOL-WING—BODY
COMBINATION UTILIZING FAVORABLE LIFT INTERFERENCE

AT MACH NUMBERS FROM 3.00 TO 4.63

By Odell A. Morris and Robert J. Mack ✓

Langley Research Center
Langley Station, Hampton, Va.

✓
NATIONAL AERONAUTICS AND SPACE ADMINISTRATION

For sale by the Clearinghouse for Federal Scientific and Technical Information
Springfield, Virginia 22151 - CFSTI price \$3.00

AERODYNAMIC CHARACTERISTICS OF A PARASOL-WING—BODY
COMBINATION UTILIZING FAVORABLE LIFT INTERFERENCE
AT MACH NUMBERS FROM 3.00 TO 4.63

By Odell A. Morris and Robert J. Mack
Langley Research Center

SUMMARY

An investigation has been conducted in the Langley Unitary Plan wind tunnel at Mach numbers from 3.00 to 4.63 to determine the longitudinal aerodynamic characteristics of a parasol-wing—body model. The model had a swept wing with a curved leading edge and a body with circular cross sections and a Von Karman forebody shape. Variations in wing position and forebody shape were also studied.

Results of the investigation show that large favorable lift interferences were obtained at zero angle of attack for all configurations with the largest interference values being measured at Mach numbers from 4.00 to 4.63 in tests of the low, single strut configuration. Variation in wing vertical position from a high to a low position improved the interference lift increments at the higher Mach numbers (4.00 to 4.63) with a corresponding increase in the maximum values of the lift-drag ratio. Variations in forebody shape from the basic body resulted in only small changes in the maximum values of the lift-drag ratio. Theoretical calculations of the lift-drag curve for the basic configuration at a Mach number of 3.00 showed good agreement with the experimental data.

INTRODUCTION

Many studies have been made in recent years concerning the favorable lift interference in supersonic flow (refs. 1 to 6). Some of the earlier studies were directed toward ring-wing and half-ring-wing—body configurations as a means of reducing wave drag (refs. 1 to 4). Results reported in references 3 and 4 indicate that the half-ring-wing—body configuration has higher lift-drag ratios than the complete-ring-wing—body configuration as a result of lower skin-friction drag and favorable lift interference produced only on the half-wing by the body. The investigation of reference 5 indicates that a flat wing strut mounted above a body also provides sizeable favorable lift interference from the body and has higher performance levels than a modified half-ring-wing configuration. Theoretical calculations based on a flat-wing configuration using recently developed high-speed computer programs indicate that further improvements in lift-drag ratios may be

obtained by using a similar model with a more conventional body shape than the broad flat body employed in the investigation of reference 5. The theory indicated that the increased performance would result from lower skin-friction drag, improved area distribution, and increased favorable lift interference for a model with a body having circular cross sections.

The present investigation has been made to determine the effect of favorable lift interference on the aerodynamic characteristics in pitch of a wing-body configuration which employs the same basic concepts as the configuration of reference 5. The present model has an uncambered swept wing with a curved leading edge which is strut mounted above the body. Three bodies, each of which had a minimum-drag Von Karman forebody shape, were tested with this swept wing. Variations in wing position were also studied. The tests were conducted in the Langley Unitary Plan wind tunnel at Mach numbers from 3.00 to 4.63 and over an angle-of-attack range from about -4° to 10° . Results of the investigation and a limited analysis are presented herein.

SYMBOLS

The data are referred to the stability-axis system with the moment reference point 20.80 inches (52.83 cm) rearward of the nose of the body. U.S. Customary Units are used, and the units for the International System are given parenthetically.

A	body half-width measured on horizontal axis (see fig. 1(b))
B	body half-height measured on vertical axis (see fig. 1(b))
C_D	drag coefficient, Drag/qS
$C_{D,0}$	drag coefficient at zero lift
C_L	lift coefficient, Lift/qS
$C_{L\alpha}$	lift-curve slope
C_m	pitching-moment coefficient, Pitching moment/qS \bar{c}
\bar{c}	wing reference chord, 13.44 inches (34.14 centimeters)
L/D	lift-drag ratio

$(L/D)_{\max}$	maximum lift-drag ratio
M	free-stream Mach number
$\frac{\partial C_m}{\partial C_L}$	longitudinal stability parameter
q	free-stream dynamic pressure, pounds/foot ² (newtons/meter ²)
r	radius, inches (centimeters)
S	reference wing area, 2.16 feet ² (0.201 meter ²)
x,y	coordinates, inches (centimeters)
z	vertical distance from wing chord plane to body center line, inches (centimeters) (see fig. 1(a))
α	angle of attack, degrees

Subscripts:

le	leading edge
te	trailing edge

Body designations:

B ₁	body with 15-inch (38.10 centimeters) Von Karman forebody length
B ₂	body with 18-inch (45.72 centimeters) modified Von Karman forebody length
B ₃	body with 18-inch (45.72 centimeters) Von Karman forebody length

MODELS AND APPARATUS

Details of the model configurations are shown in figure 1 and photographs of the models are shown in figures 2 and 3. The wing had 3-percent-thick double-wedge sections and an area of 2.16 ft² (0.201 m²). The outboard panels of the curved wing had a

leading-edge sweep of 68.5° and was designed to reflect the body nose shock at a Mach number of 3.00 for the high wing position. The wing leading-edge shape was determined by the intersection of the body-generated Mach cone with a flat-plate representation of the wing surface. The forebody section of the body nose produces positive pressures which act on the wing and create favorable positive lift interference. However, as the flow approaches the body maximum diameter, expansion of the flow occurs and produces a negative pressure region. In this region the wing trailing edge was positioned so as to avoid the negative pressures acting on the wing. Coordinates for the parasol wing are listed in table I.

Three body configurations were tested. Each of the three bodies had a Von Karman minimum-drag forebody shape. Rearward of the maximum body diameter the bodies were contoured as much as possible (based on the sting-diameter limitation) to reduce wave drag. The basic body, which is designated body 3 (B₃), had an 18-in. (45.72 cm) forebody length and circular cross sections. Body 2 (B₂) also had an 18-in. (45.72 cm) forebody length but was modified to have elliptical cross sections in the region of the body center section. Body 1 (B₁) had a forebody length of 15 in. (38.10 cm) and also had circular cross sections. The coordinates for each of the body shapes are given in table II.

The wing mounting struts provided for three vertical wing positions. For the high wing and midwing positions the wing was mounted on two struts as shown in figure 1(a). These struts had a 6-in. (15.24 cm) chord width with 3-percent-thick double-wedge streamwise sections. For the low wing position a single center strut was used (fig. 1(a)). This strut had a chord length of 8.9 in. (22.61 cm) and a wedge-shaped forward section with a 14.1° total wedge angle. The thickness-chord ratio at maximum thickness was 0.14. This thickness was considered to be about the minimum width of a single strut that would provide a structurally satisfactory mount for the wing.

The wing-body models were sting mounted on a remote-control support system in the Langley Unitary Plan wind tunnel and the forces and moments were measured by means of a six-component strain-gage balance mounted within the model.

TESTS AND CORRECTIONS

The tests were made at the following conditions:

Mach number	Stagnation temperature	
	$^\circ\text{F}$	$^\circ\text{K}$
3.00	150	338
3.25	150	338
3.50	150	338
4.00	175	353
4.63	175	353

The dewpoint was held sufficiently low to prevent measurable condensation effects in the test section. Tests were made through an angle-of-attack range from about -4° to 10° at a Reynolds number of 3.0×10^6 per foot (9.8×10^6 per meter). The angles of attack were corrected for deflection of the balance-sting combination under load and for tunnel flow angularity. The balance-chamber pressures were measured and the drag forces were adjusted to correspond to a condition of free-stream static pressure at the model base. To provide turbulent boundary-layer conditions on the model, transition strips of No. 40 carborundum grit were applied 0.5 in. (1.27 cm), measured streamwise, from the nose of the body and the leading edges of the wing and struts.

RESULTS AND DISCUSSION

The data of figure 4 show the effect of wing vertical position on the aerodynamic characteristics in pitch of the configuration with the basic body (body 3). The effect of body shape on the aerodynamic characteristics in pitch for the high wing vertical position is shown in figure 5. Results from these basic data plots are summarized in figures 6 and 7 which show the variation of several longitudinal parameters over the Mach number range.

Figure 6 shows that a maximum L/D value of about 6.8 is obtained at the design Mach number of 3.00 for the high wing position ($z/\bar{c} = 0.253$). In general, a slight reduction in the values of $(L/D)_{\max}$ occurs with increasing Mach number for the high wing and midwing positions, but for the low wing position the values of $(L/D)_{\max}$ are nearly constant throughout the Mach number range. The L/D values at an angle of attack of zero are a measure of the favorable lift interference produced by the body on the wing. In the high Mach number range ($M = 4.00$ to 4.63), variation in wing vertical position from a high to a low position improved the interference lift increments and maximum lift-drag ratios so that the largest values of $(L/D)_{\alpha = 0}$ are shown to occur for the low wing position. The larger interference values for the low wing position are probably due to the fact that the single wedged-shape strut also produces favorable lift interference on the wing in addition to that produced by the forebody pressures acting on the wing. However, for the low wing position the full effect of the body pressures acting on the wing is not obtained at the lower Mach numbers. Increasing the Mach number to 4.63 decreased the Mach angle to such an extent that the largest part of the body pressure field was reflected by the wing.

Increasing the model angle of attack moves the shock forward of the wing and the favorable interference lift produced by the body pressures on the wing is gradually decreased. At a Mach number of 4.63 the Mach angle has decreased to such an extent that variation in model angle of attack appears to cause a more rapid decrease in interference lift than occurs at the lower Mach numbers. Thus, the interference lift obtained at $\alpha = 0^{\circ}$ for the high Mach numbers is not proportionally reflected in the values of $(L/D)_{\max}$ obtained (note that $(L/D)_{\max}$ occurs at $\alpha \approx 4^{\circ}$). To determine the full extent of the

benefits of such interference effects in this Mach number range, the wing would have to be designed for the higher Mach number and would probably require twist and camber to provide a cruise lift coefficient sufficient to maintain the forebody angle of attack at or near 0° .

The effects of body shape with the high wing positions are summarized in figure 7. In general, no large changes were noted in the longitudinal parameters $C_{L\alpha}$, $\frac{\partial C_m}{\partial C_L}$, and $C_{D,0}$ due to body shape. The maximum L/D values were about the same at $M = 3.00$ for bodies 2 and 3. As the Mach number was increased, body 2 had slightly higher L/D values than bodies 1 and 3 (basic). These values were apparently due to slightly lower values of minimum drag for body 2 which were obtained at the expense of a reduced body cross-sectional area in the region of maximum diameter (fig. 1(b)).

A comparison of theoretical and experimental lift and drag data at a Mach number of 3.00 for the high wing model is presented in figure 8. The theoretical values were calculated by means of several available high-speed computer programs either reported in or based on references 7, 8, and 9. The body interference effects on the wing were calculated by using a computer program based on Whitham's modified linear theory. Good agreement is seen between the theoretical and experimental results. No adjustment to the tunnel data was made for grit drag which is usually very small. However, a small correction, if applied to the tunnel data, would tend to further improve the agreement between theory and experiment.

CONCLUSIONS

An investigation has been conducted in the Langley Unitary Plan wind tunnel at Mach numbers from 3.00 to 4.63 to determine the aerodynamic characteristics in pitch of a parasol-wing—body model. The investigation also included tests on the model with variations in wing vertical position and forebody shape. The following conclusions were indicated:

1. Favorable lift interferences were obtained at 0° angle of attack for all parasol-wing—body configurations with the largest interference values being measured at Mach numbers from 4.00 to 4.63 in tests with the low wing position.

2. Variation in wing vertical position from a high to a low position improved the interference lift increments at the higher Mach numbers (4.00 to 4.63) with a corresponding increase in the maximum values of lift-drag ratio.

3. Changes in forebody shape from that of the basic body resulted in small changes in the maximum values of the lift-drag ratio.

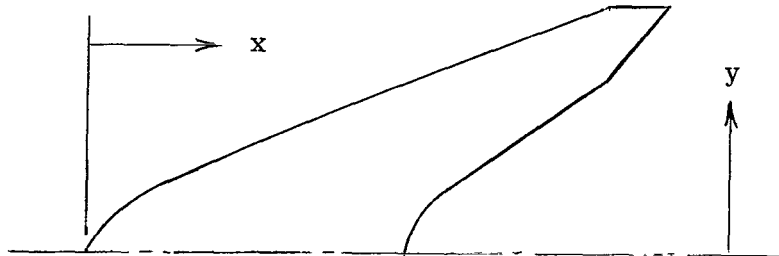
4. Theoretical calculations of the lift-drag curve for the basic configurations at a Mach number of 3.00 showed good agreement with the experimental data.

Langley Research Center,
National Aeronautics and Space Administration,
Langley Station, Hampton, Va., June 21, 1968,
126-13-02-08-23.

REFERENCES

1. Johnson, Roger P.: Verification of Ring-Wing Theory. U.S. Air Force Proj. RAND Briefing B-224, The RAND Corp., Jan. 4, 1961.
2. Browand, Frederick K.; Beane, Beverly J.; and Nowlan, Daniel T.: The Design and Test at Mach Number 2.5 of Two Low-Wave-Drag Ring-Wing Configurations of Aspect Ratio 1.3 and 2.6. RM-2933-PR, The RAND Corp., June 1962.
3. Morris, Odell: Aerodynamic Characteristics in Pitch of Several Ring-Wing—Body Configurations at a Mach Number of 2.2. NASA TN D-1272, 1962.
4. Moore, K. C.; and Jones, J. G.: Some Aspects of the Design of Half-Ring Wing—Body Combinations With Prescribed Wing Loadings. Tech. Note No. Aero 2860, Brit. R.A.E., Dec. 1962.
5. Morris, Odell A.; and Lamb, Milton: Aerodynamic Characteristics in Pitch of a Modified-Half-Ring-Wing—Body Combination and a Swept-Wing—Body Combination at Mach 2.16 to 3.70. NASA TM X-1551, 1968.
6. Boyd, J. A.: Optimal Utilization of Supersonic Favorable Interference To Obtain High Lift-Drag Ratios. AIAA Paper No. 65-752, Nov. 1965.
7. Harris, Roy V., Jr.: An Analysis and Correlation of Aircraft Wave Drag. NASA TM X-947, 1964.
8. Sommer, Simon C.; and Short, Barbara J.: Free-Flight Measurements of Turbulent-Boundary-Layer Skin Friction in the Presence of Severe Aerodynamic Heating at Mach Numbers From 2.8 to 7.0. NACA TN 3391, 1955.
9. Middleton, Wilbur D.; and Carlson, Harry W.: A Numerical Method for Calculating the Flat-Plate Pressure Distributions on Supersonic Wings of Arbitrary Planform. NASA TN D-2570, 1965.

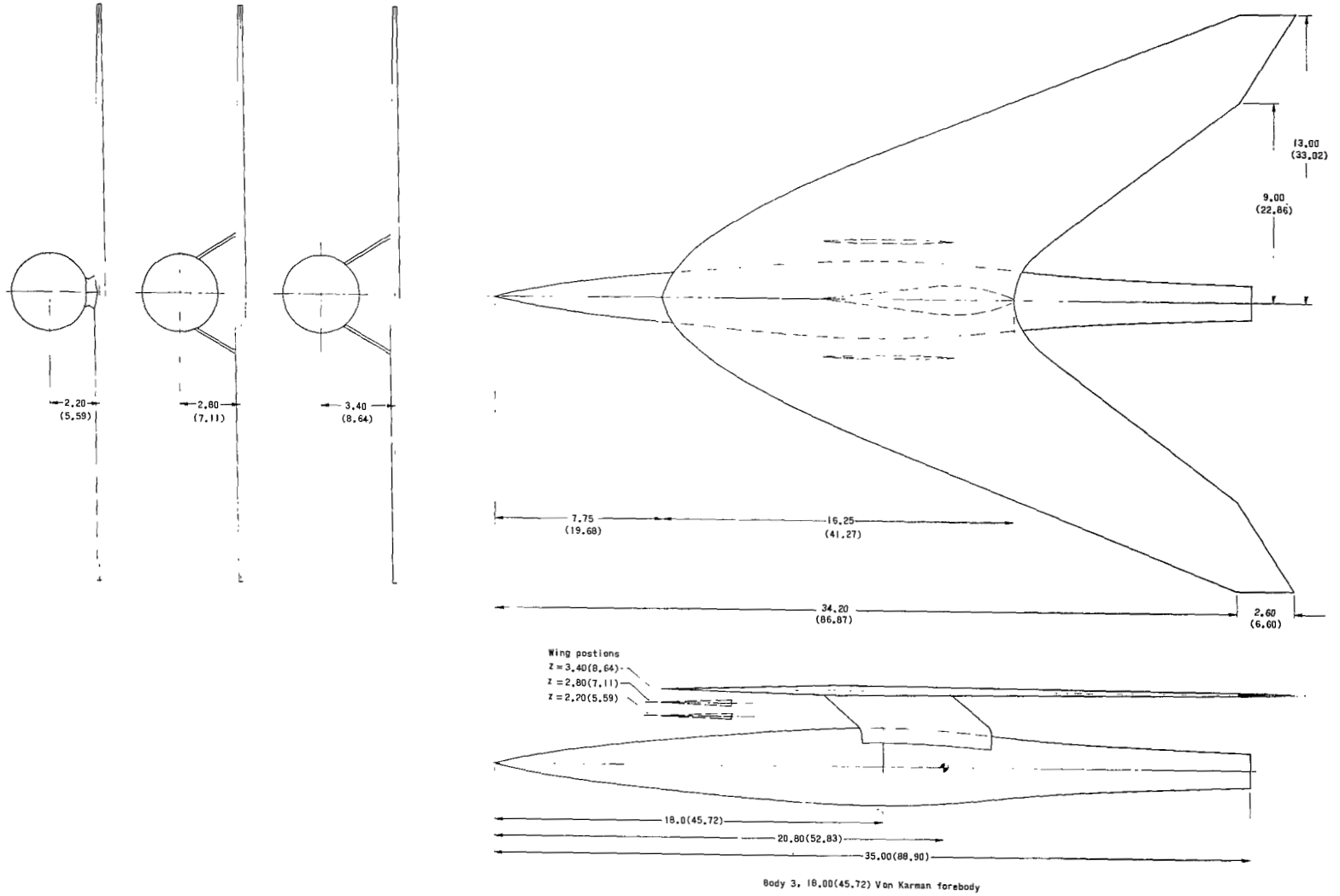
TABLE I.- COORDINATES OF PARASOL WING



y		x_{le}		x_{te}	
in.	cm	in.	cm	in.	cm
0	0	0	0	16.25	41.28
.32	.81	.10	.25	16.30	41.40
.65	1.65	.25	.64	16.37	41.57
.97	2.46	.42	1.07	16.49	41.88
1.30	3.30	.65	1.65	16.55	42.04
1.95	4.95	1.20	3.05	17.13	43.51
2.60	6.60	1.98	5.03	17.97	45.64
3.25	8.25	2.95	7.49	18.84	47.85
3.90	9.90	4.08	10.36	19.70	50.04
4.55	11.56	5.30	13.46	20.58	52.27
5.20	13.21	6.67	16.94	21.43	54.43
5.85	14.86	8.19	20.80	22.31	56.67
6.50	16.51	9.83	24.97	23.17	58.85
7.15	18.16	11.50	29.21	24.04	61.06
7.80	19.81	13.16	33.43	24.90	63.25
8.45	21.46	14.83	37.67	25.75	65.40
9.00	22.86	16.25	41.27	26.50	67.31
9.42	23.93	17.33	44.02	26.77	67.99
10.07	25.58	19.00	48.26	27.18	69.04
10.72	27.23	20.66	52.48	27.60	70.10
11.37	28.88	22.33	56.72	28.02	71.17
12.02	30.53	23.98	60.91	28.44	72.24
13.00	33.02	26.45	67.18	29.05	73.79

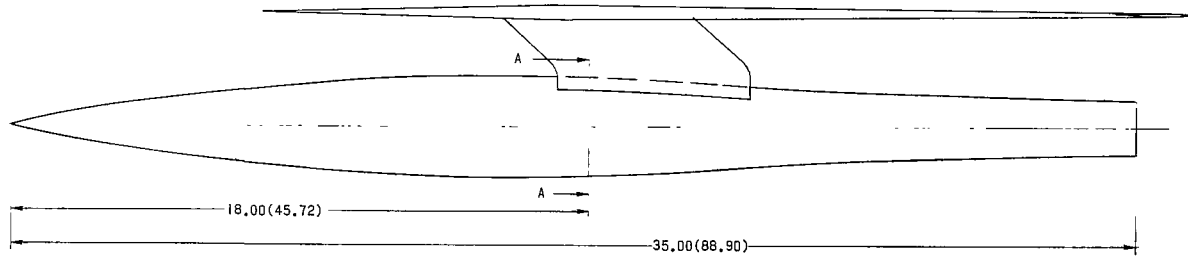
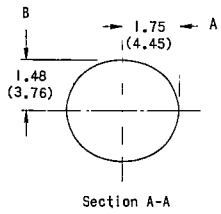
TABLE II. - COORDINATES OF TEST BODIES

x		Body 1		Body 3		Body 2			
		r		r		A		B	
in.	cm	in.	cm	in.	cm	in.	cm	in.	cm
0	0	0	0	0	0	0	0	0	0
.50	1.27	.177	.449	.154	.391	.154	.391	.154	.391
1.00	2.54	.296	.752	.259	.658	.259	.658	.259	.658
1.50	3.81	.399	1.013	.349	.886	.349	.886	.349	.886
2.00	5.08	.493	1.252	.431	1.095	.431	1.095	.431	1.095
2.50	6.35	.579	1.471	.508	1.290	.508	1.290	.508	1.290
3.00	7.62	.660	1.676	.579	1.471	.579	1.471	.579	1.471
3.50	8.89	.737	1.872	.647	1.643	.647	1.643	.647	1.643
4.00	10.16	.810	2.057	.712	1.808	.712	1.808	.712	1.808
4.50	11.43	.879	2.233	.774	1.966	.774	1.966	.774	1.966
5.00	12.70	.945	2.400	.833	2.116	.833	2.116	.833	2.116
5.50	13.97	1.009	2.563	.890	2.261	.890	2.261	.890	2.261
6.00	15.24	1.070	2.719	.945	2.400	.945	2.400	.945	2.400
6.50	16.51	1.128	2.865	.998	2.535	.998	2.535	.998	2.535
7.00	17.78	1.184	3.007	1.050	2.667	1.050	2.667	1.050	2.667
7.50	19.05	1.237	3.142	1.099	2.791	1.099	2.791	1.099	2.791
8.00	20.32	1.289	3.274	1.147	2.913	1.147	2.913	1.147	2.913
8.50	21.59	1.338	3.401	1.193	3.030	1.193	3.030	1.193	3.030
9.00	22.86	1.385	3.518	1.237	3.142	1.237	3.142	1.237	3.142
9.50	24.13	1.430	3.632	1.280	3.251	1.280	3.251	1.280	3.251
10.00	25.40	1.473	3.741	1.322	3.359	1.322	3.359	1.322	3.359
10.50	26.67	1.513	3.843	1.362	3.459	1.362	3.459	1.362	3.459
11.00	27.94	1.551	3.939	1.400	3.556	1.400	3.556	1.400	3.556
12.00	30.48	1.621	4.117	1.473	3.741	1.473	3.741	1.458	3.703
13.00	33.02	1.679	4.265	1.539	3.909	1.539	3.909	1.495	3.797
14.00	35.56	1.725	4.381	1.599	4.061	1.599	4.061	1.517	3.853
15.00	38.10	1.750	4.445	1.651	4.194	1.651	4.194	1.523	3.868
16.00	40.64	1.743	4.427	1.696	4.308	1.696	4.308	1.510	3.835
17.00	43.18	1.715	4.356	1.731	4.397	1.731	4.397	1.493	3.792
18.00	45.72	1.668	4.236	1.750	4.445	1.750	4.445	1.482	3.764
19.00	48.26	1.599	4.061	1.739	4.417	1.739	4.417	1.461	3.711
20.00	50.80	1.519	3.858	1.698	4.313	1.698	4.313	1.415	3.594
21.00	53.34	1.424	3.617	1.622	4.120	1.622	4.120	1.342	3.409
22.00	55.88	1.333	3.386	1.526	3.876	1.526	3.876	1.264	3.211
23.00	58.42	1.249	3.172	1.421	3.609	1.421	3.609	1.205	3.061
24.00	60.96	1.173	2.979	1.323	3.360	1.323	3.360	1.124	2.855
25.00	63.50	1.118	2.840	1.239	3.147	1.239	3.147	1.079	2.741
26.00	66.04	1.070	2.718	1.170	2.972	1.170	2.972	1.039	2.639
27.00	68.58	1.031	2.619	1.109	2.817	1.109	2.817	1.005	2.553
28.00	71.12	.993	2.522	1.050	2.667	1.050	2.667	.986	2.504
29.00	73.66	.961	2.441	.990	2.515	.990	2.515	.949	2.410
30.00	76.20	.927	2.355	.938	2.383	.938	2.383	.926	2.352
31.00	78.74	.897	2.278	.897	2.278	.897	2.278	.897	2.278
32.00	81.28	.870	2.210	.870	2.210	.870	2.210	.870	2.210
33.00	83.82	.845	2.146	.845	2.146	.845	2.146	.845	2.146
34.00	86.36	.820	2.083	.820	2.083	.820	2.083	.820	2.083
35.00	88.90	.800	2.032	.800	2.032	.800	2.032	.800	2.032

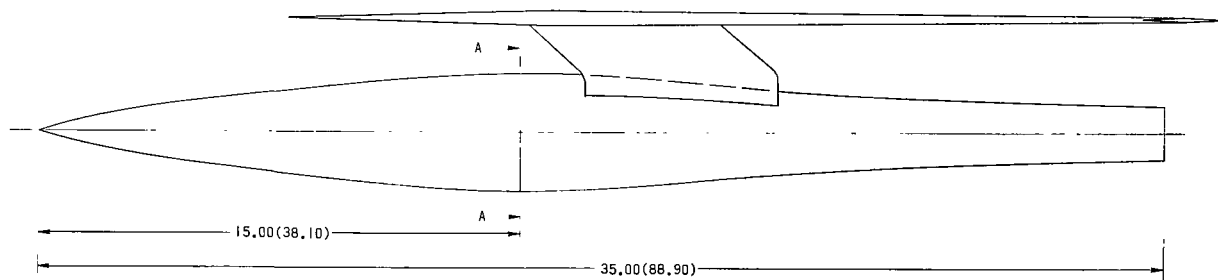
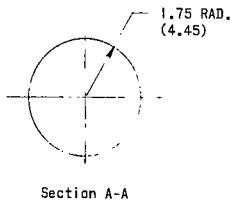


(a) Basic parasol-wing-body model.

Figure 1.- Details of models. All linear dimensions are given in inches and parenthetically in centimeters.



Body 2, modified Von Karman forebody



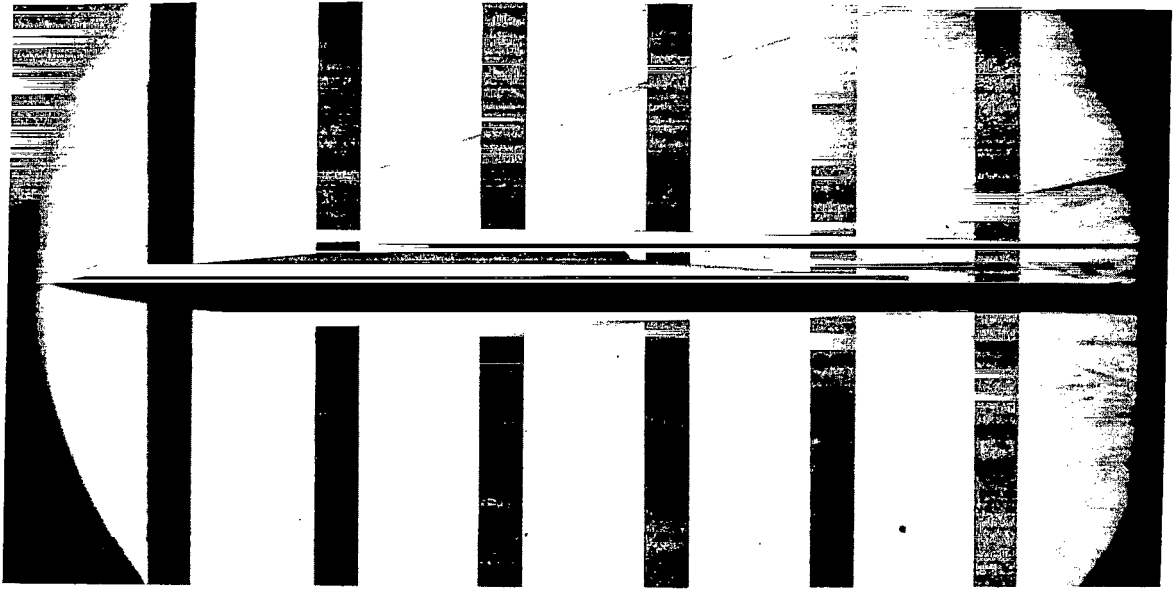
Body 1, Von Karman forebody

(b) Bodies 1 and 2.

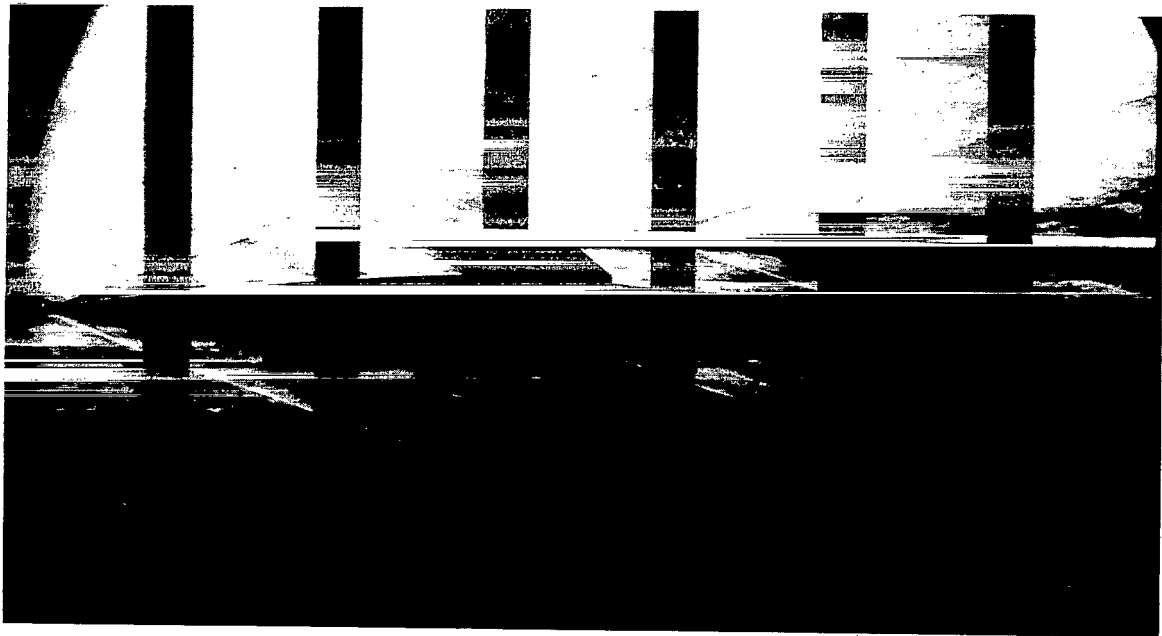
Figure 1.- Concluded.



Figure 2.- Model in Langley Unitary Plan wind tunnel.



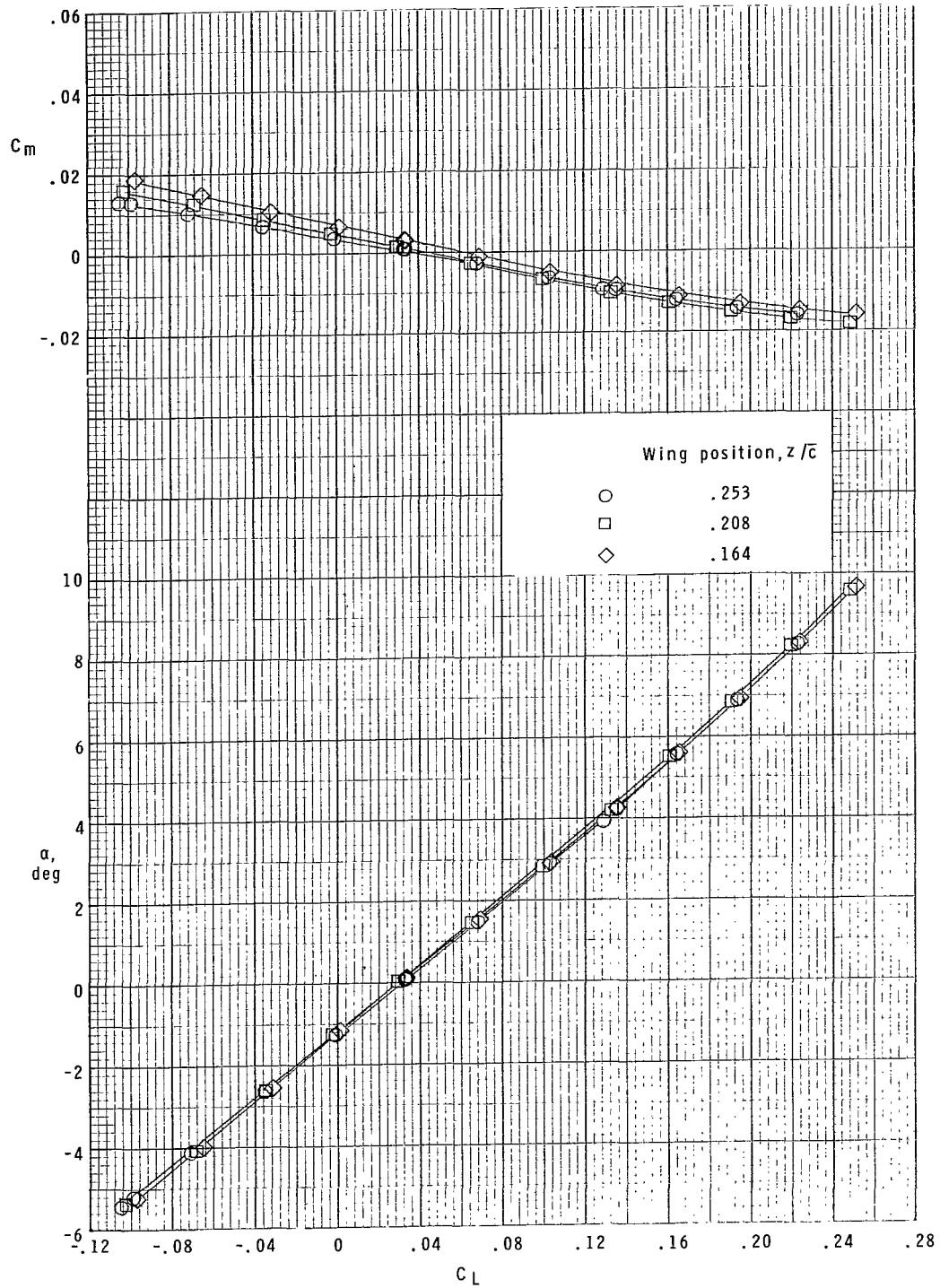
(a) Body 3 with wing in low position.



(b) Body 3 with wing in high position.

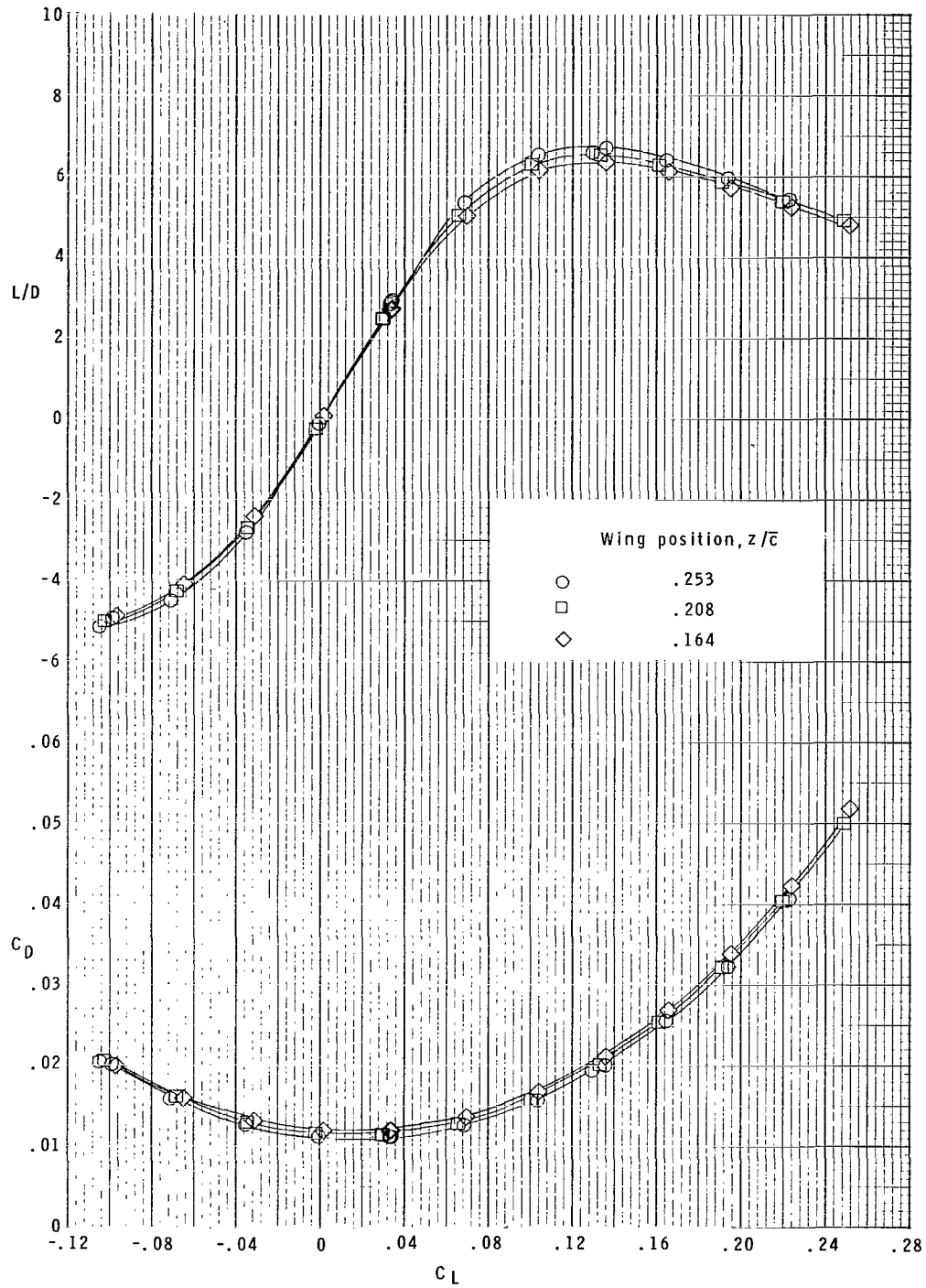
L-68-5662

Figure 3.- Schlieren photographs of model at $M = 3.25$ and $\alpha = 0$.



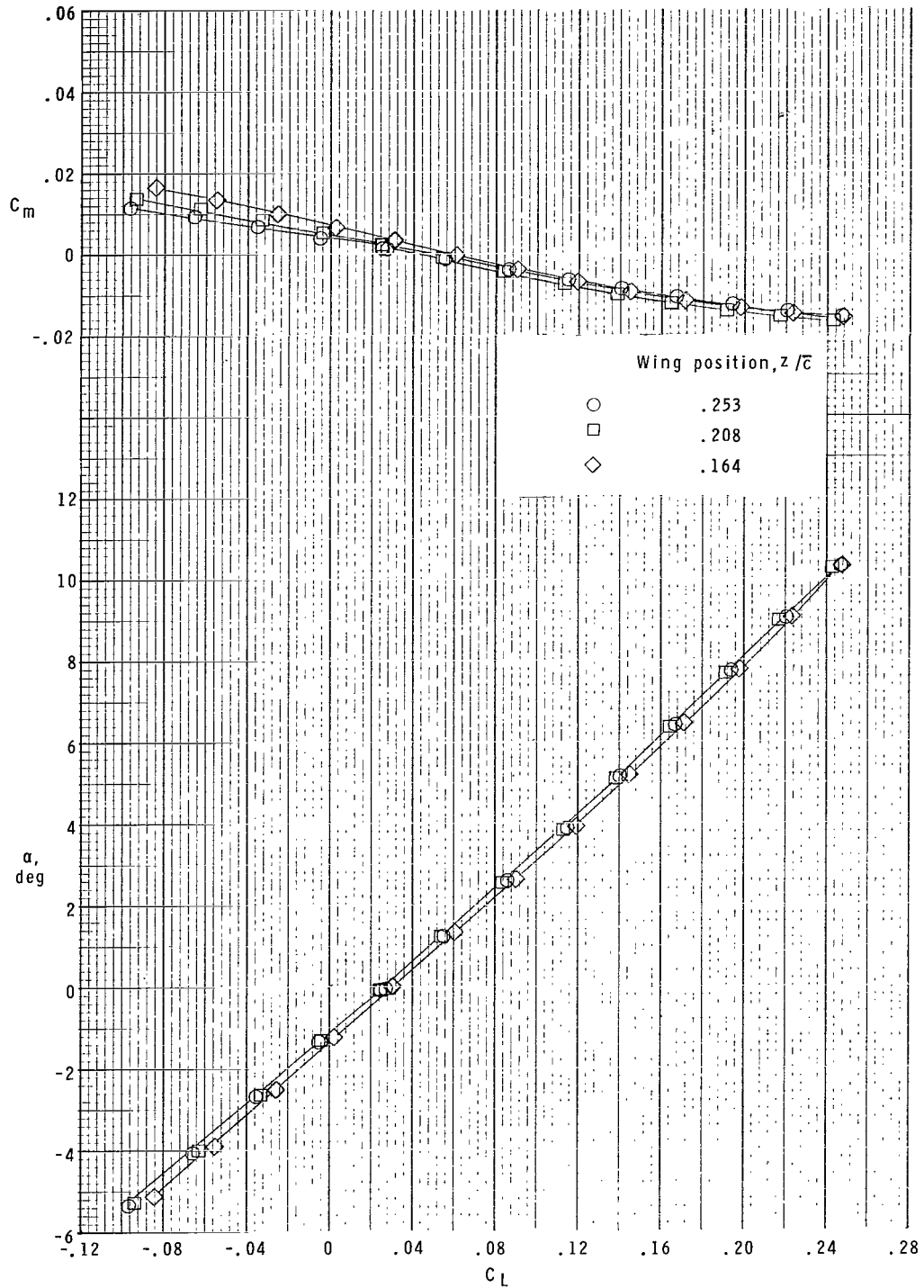
(a) $M = 3.00$.

Figure 4.- Effect of wing vertical position on the aerodynamic characteristics in pitch of the model with body 3.



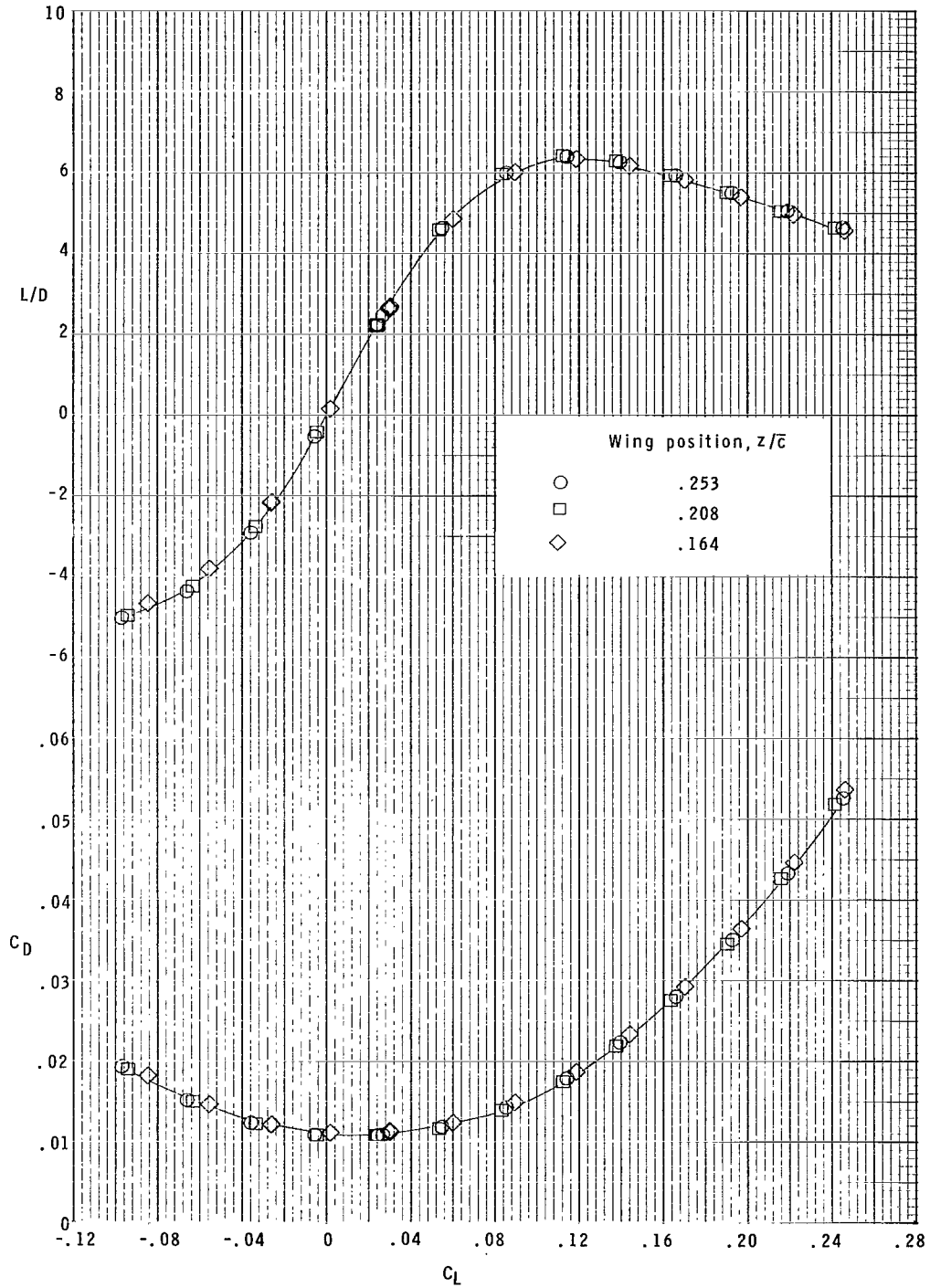
(a) Concluded.

Figure 4.- Continued.

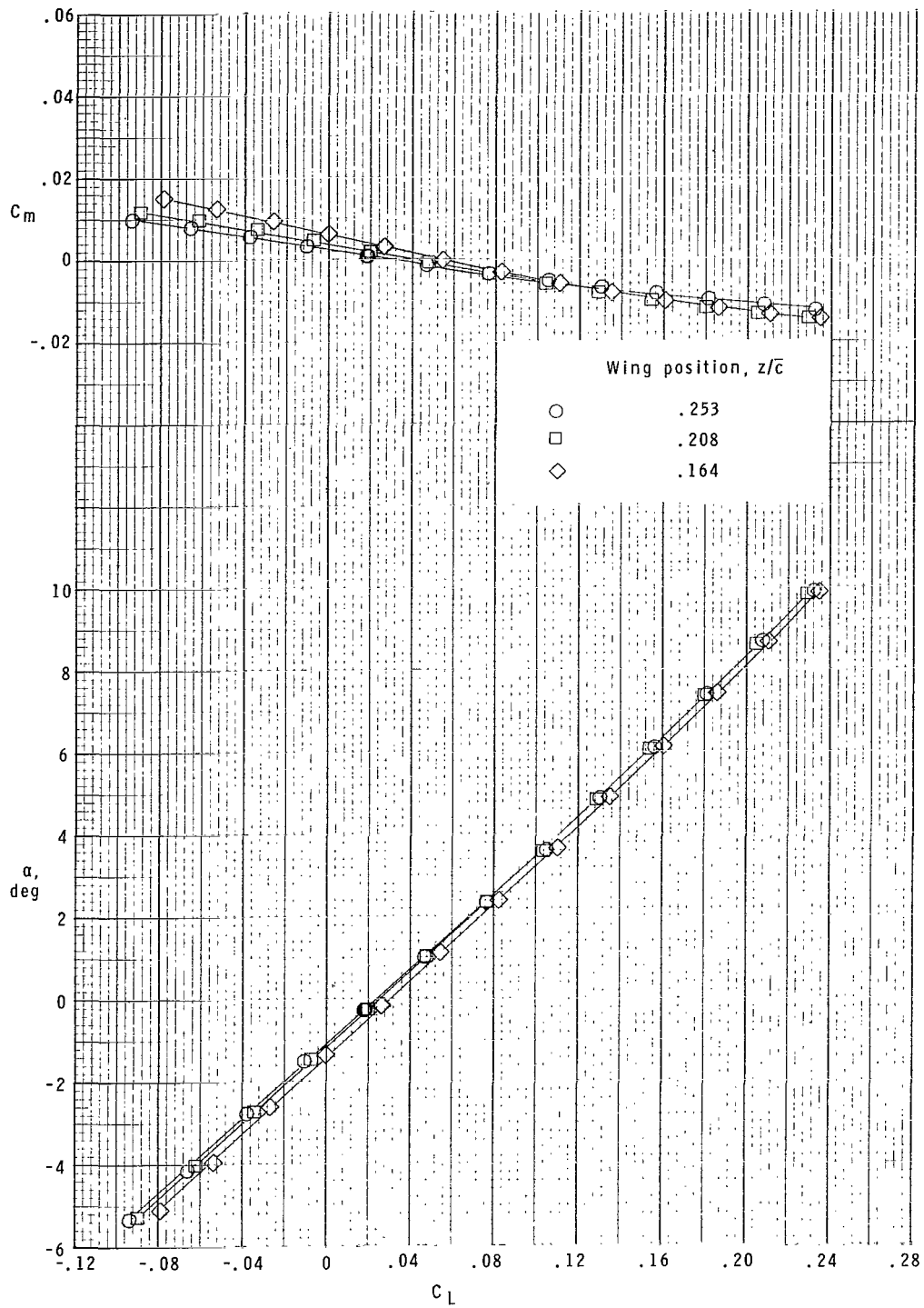


(b) $M = 3.25$.

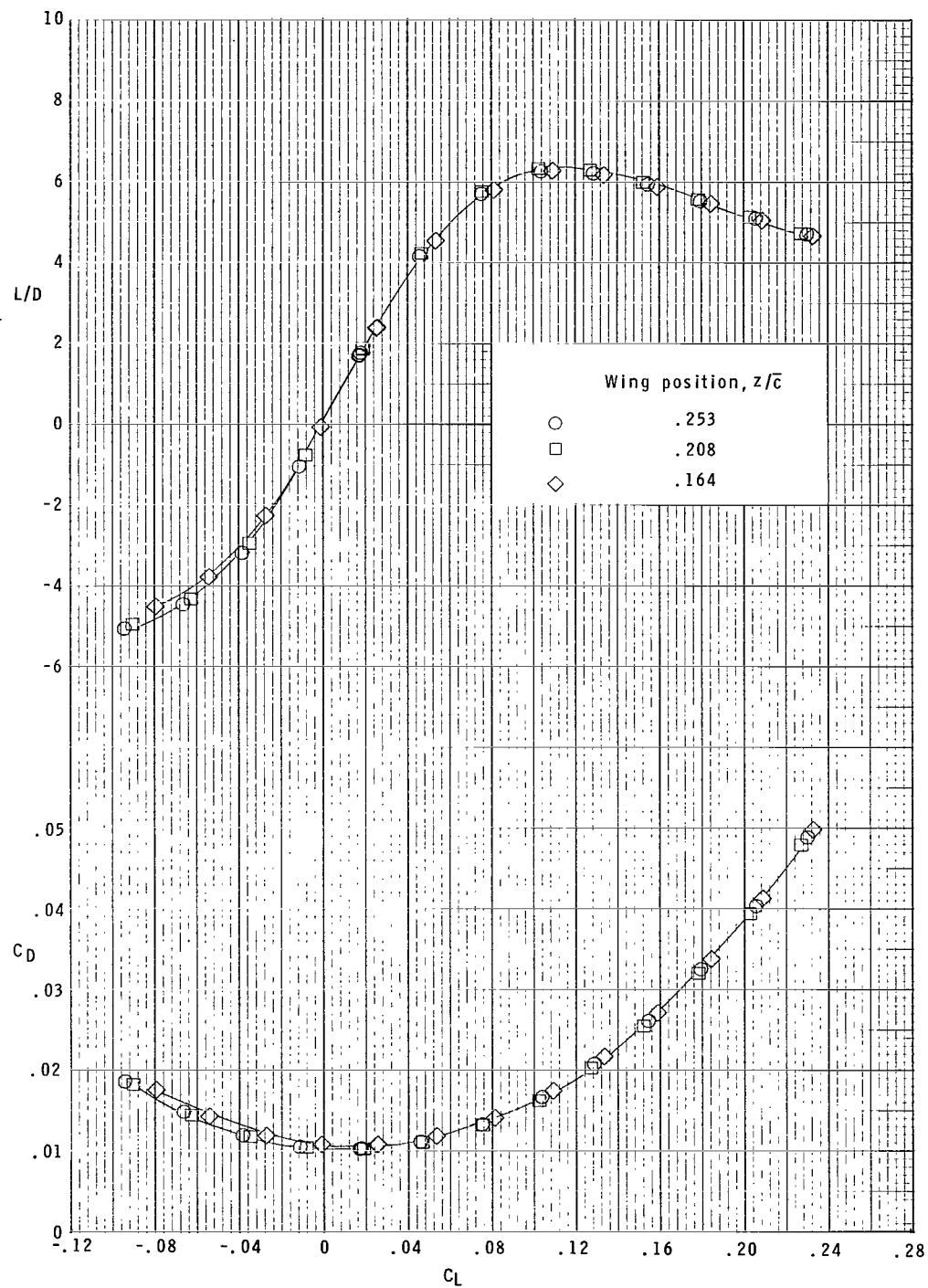
Figure 4.- Continued.



(b) Concluded.
 Figure 4.-Continued.

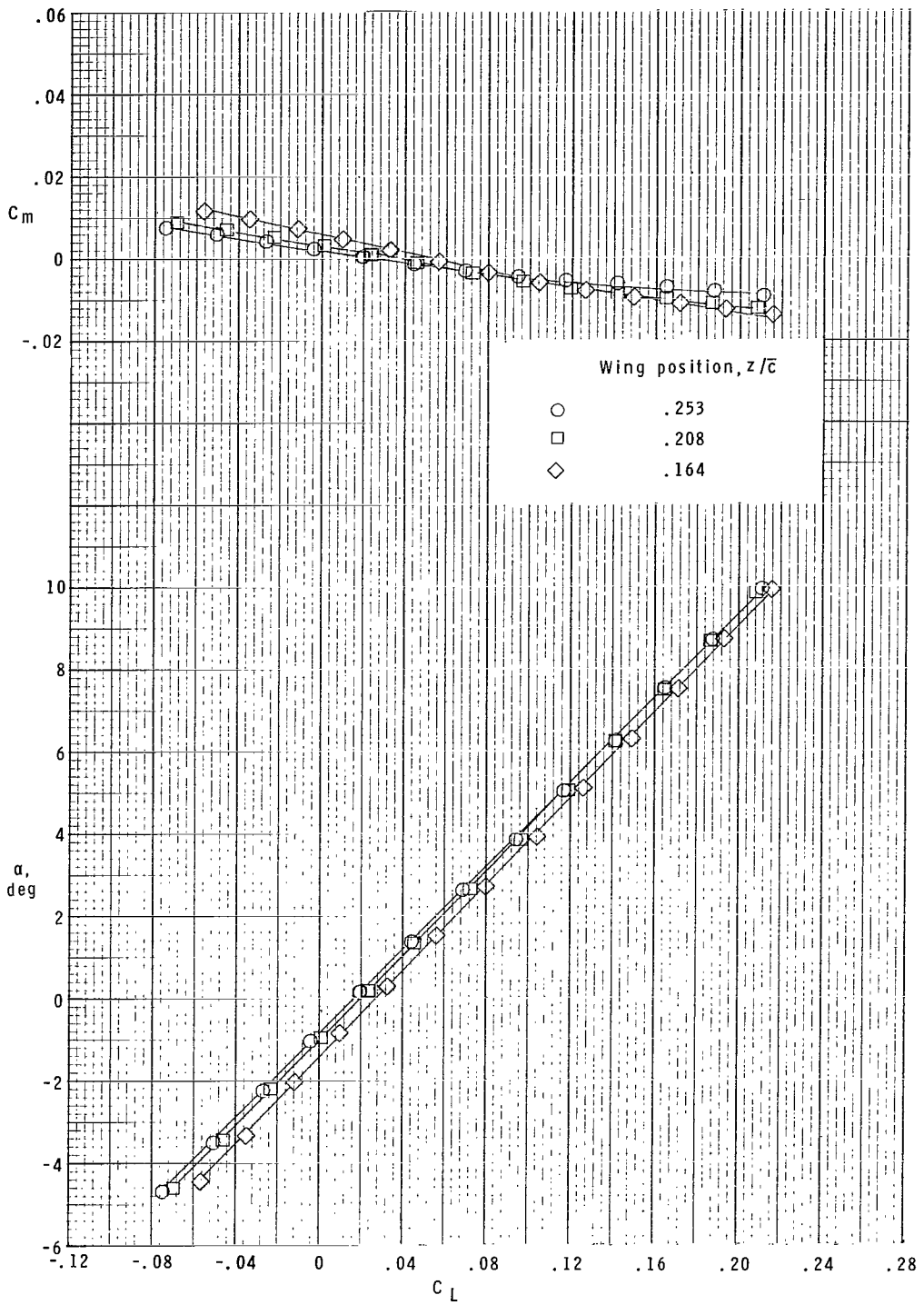


(c) $M = 3.50$.
 Figure 4.-Continued.



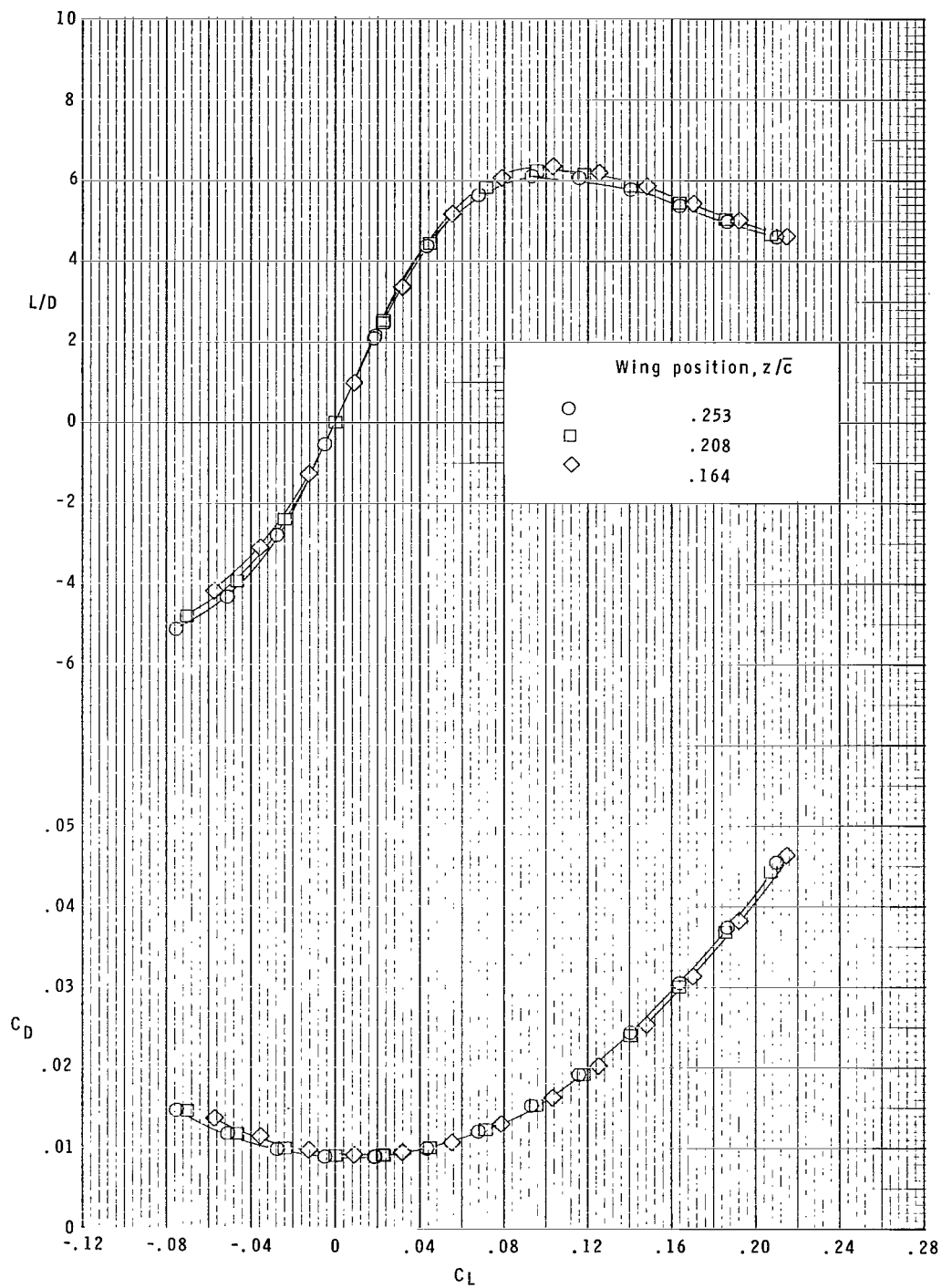
(c) Concluded.

Figure 4.- Continued.



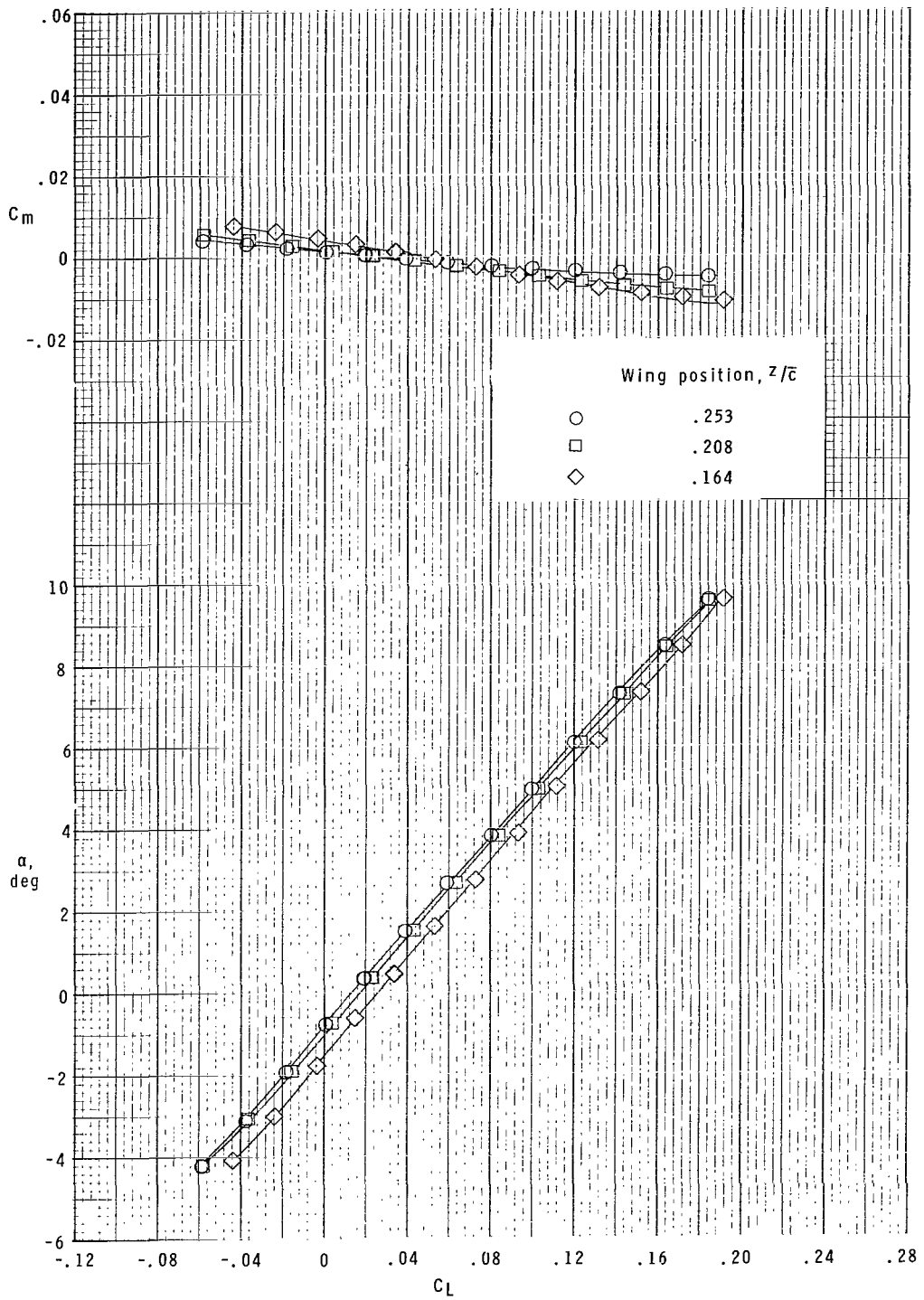
(d) $M = 4.00$.

Figure 4.- Continued.



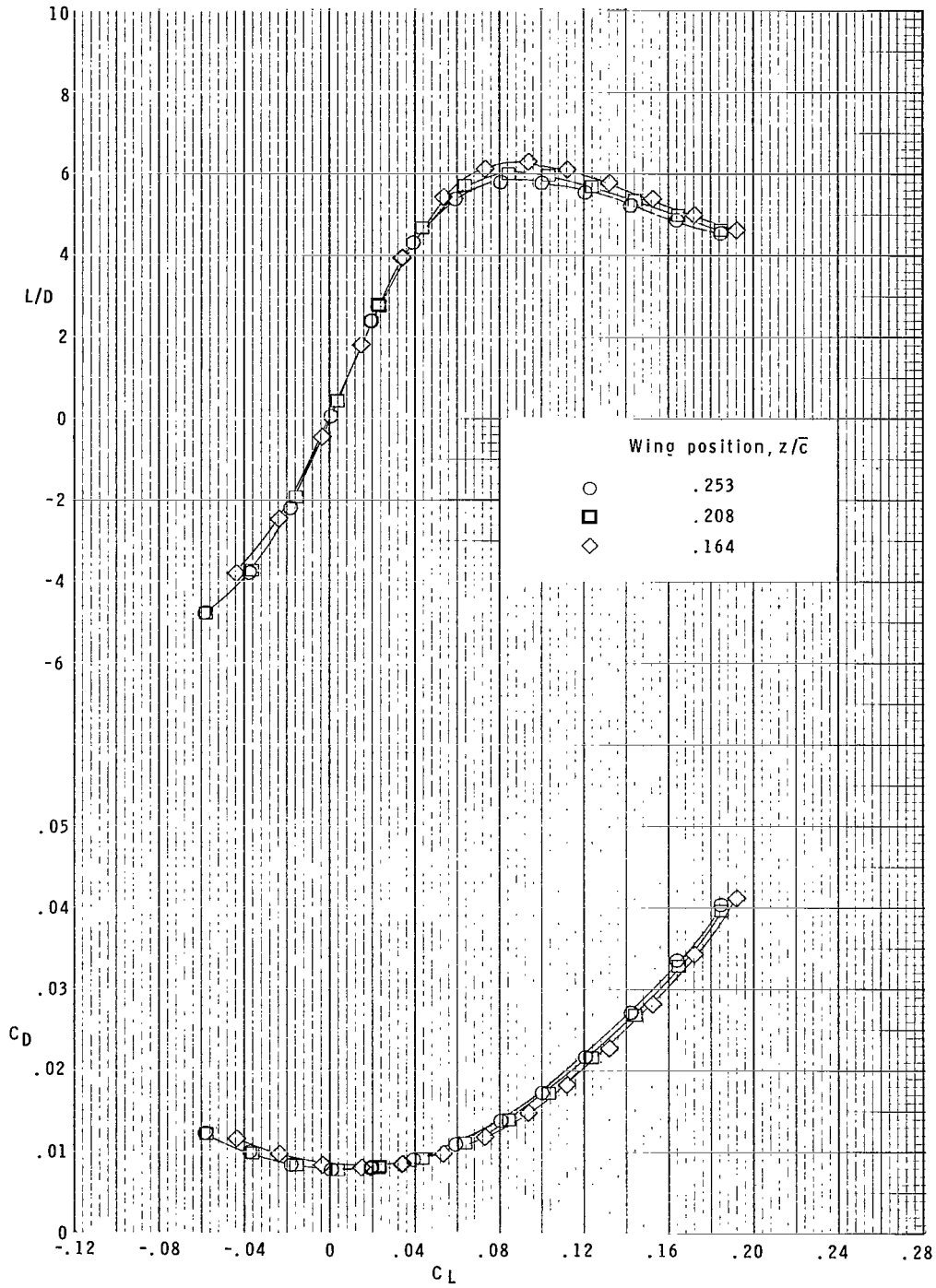
(d) Concluded.

Figure 4.- Continued.



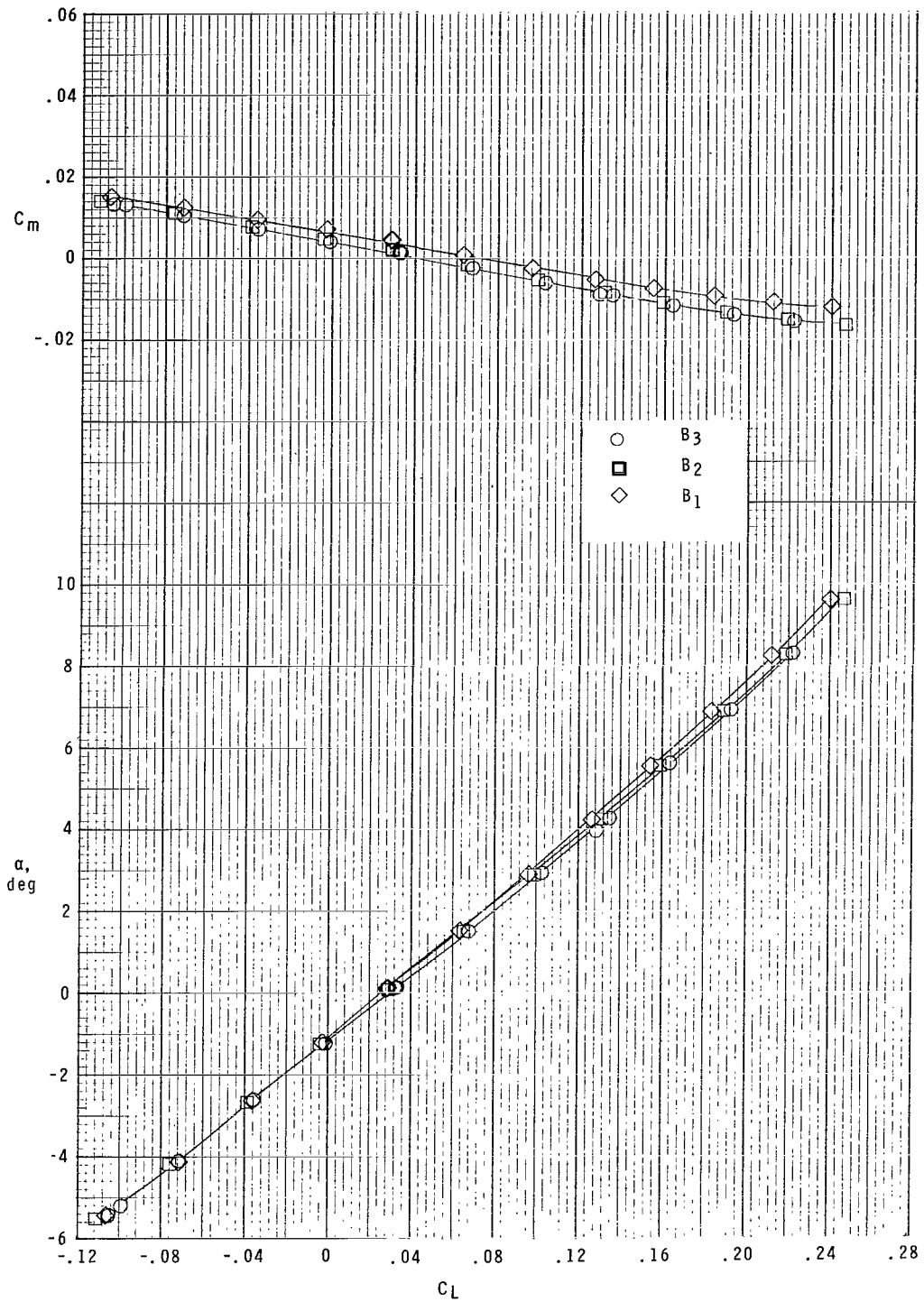
(e) $M = 4.63$.

Figure 4.- Continued.



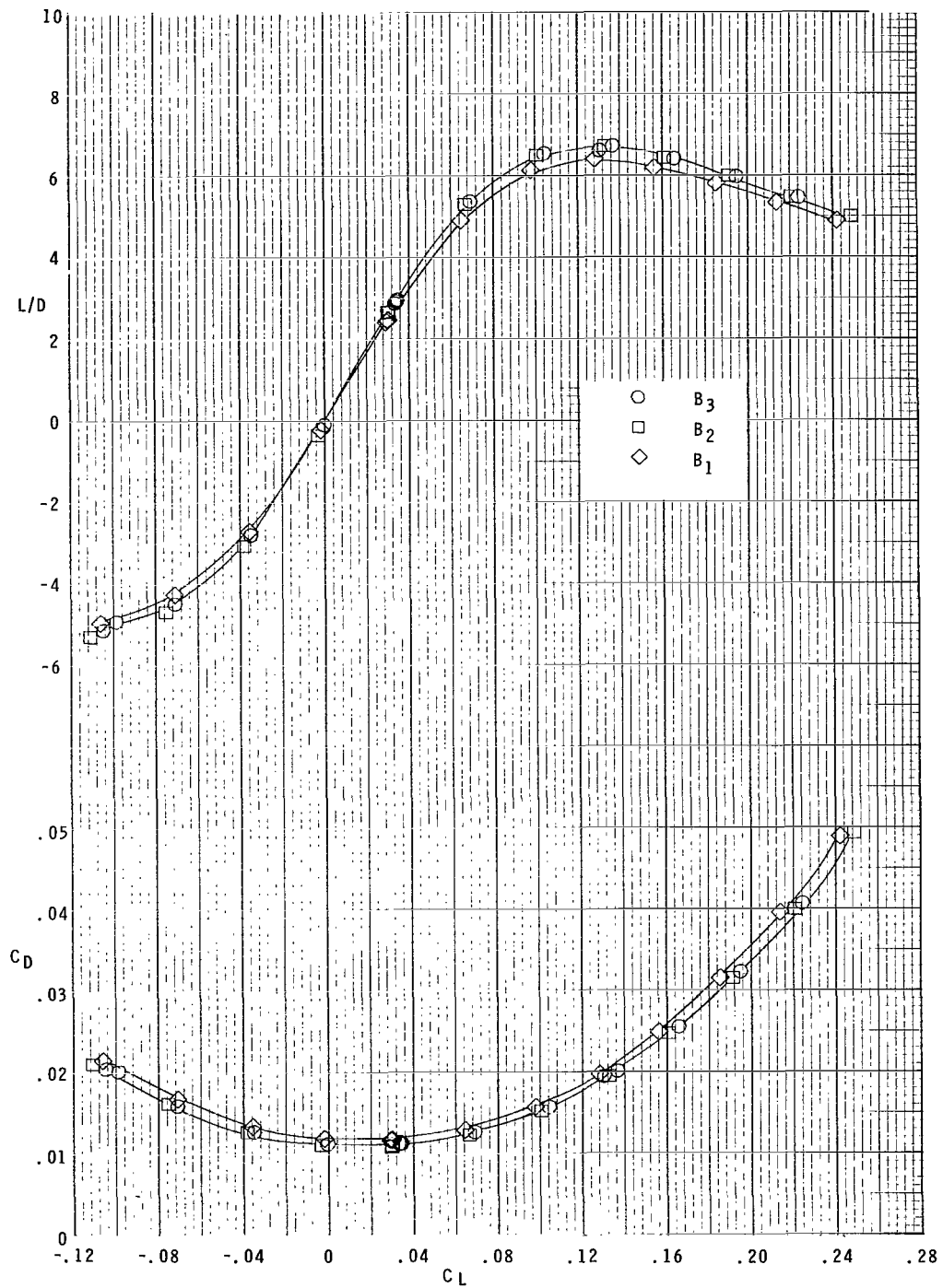
(e) Concluded.

Figure 4.- Concluded.



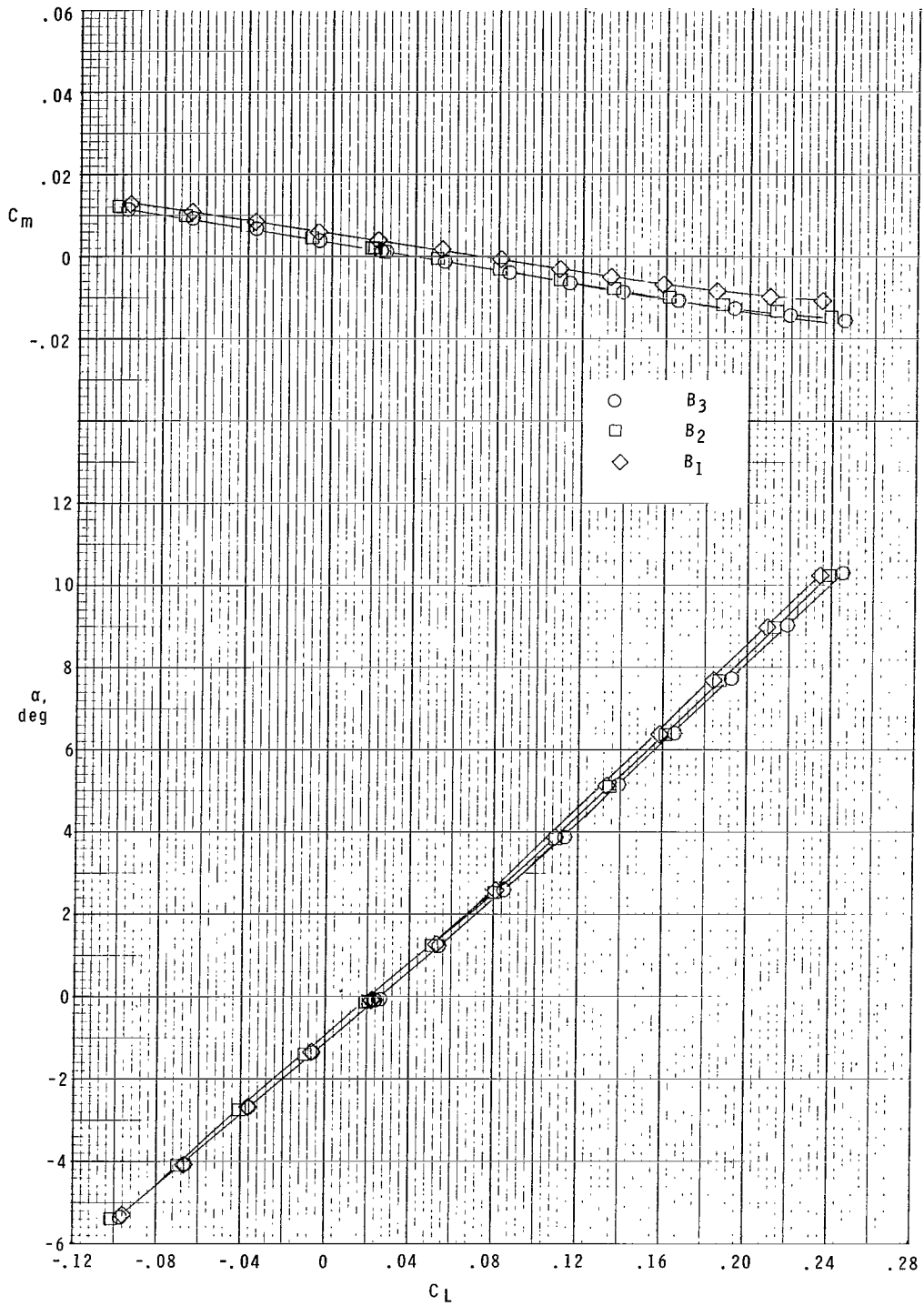
(a) $M = 3.00$.

Figure 5.- Effect of body shape on the aerodynamic characteristics in pitch of the model with wing in the high position.



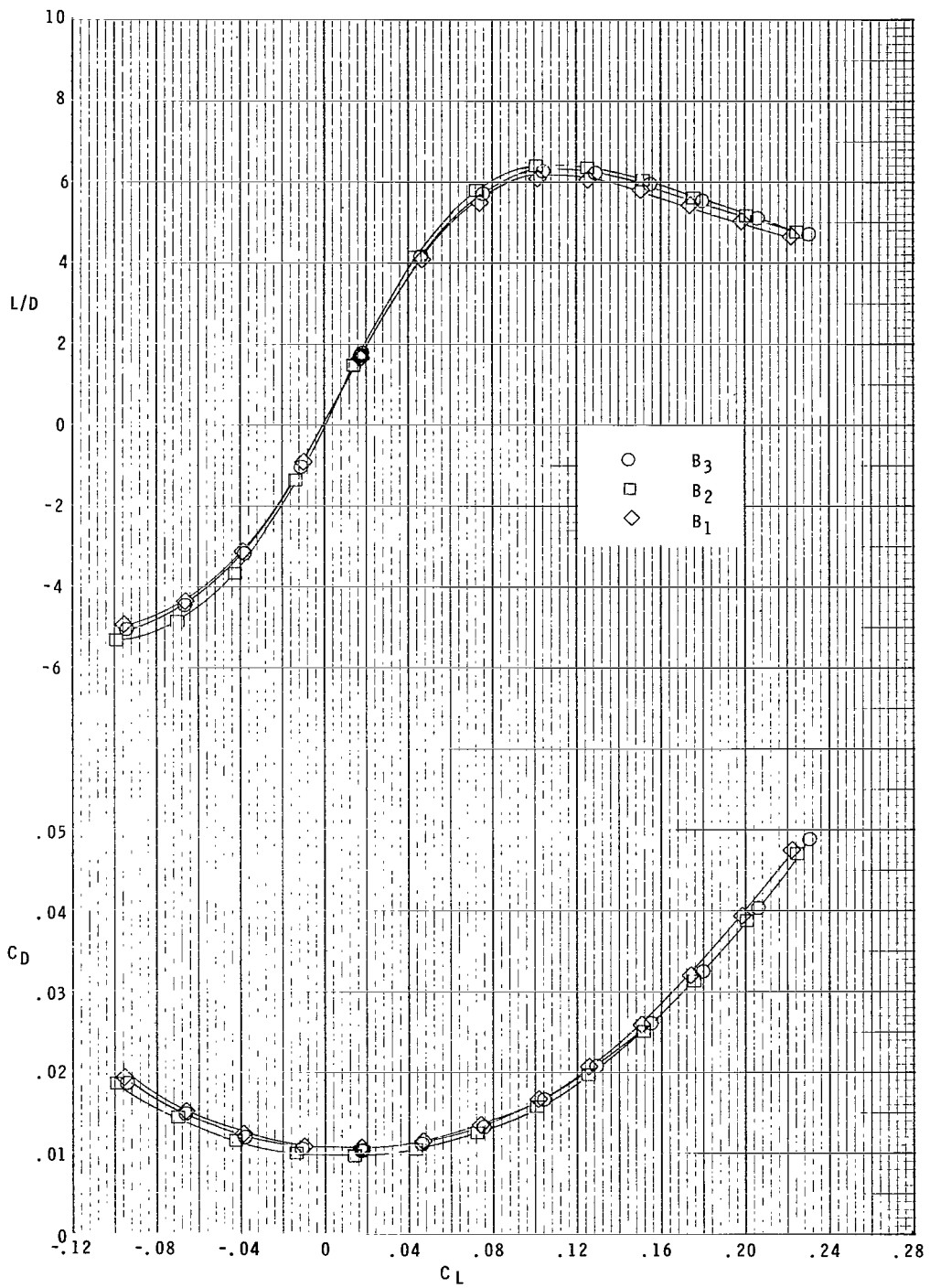
(a) Concluded.

Figure 5.- Continued.



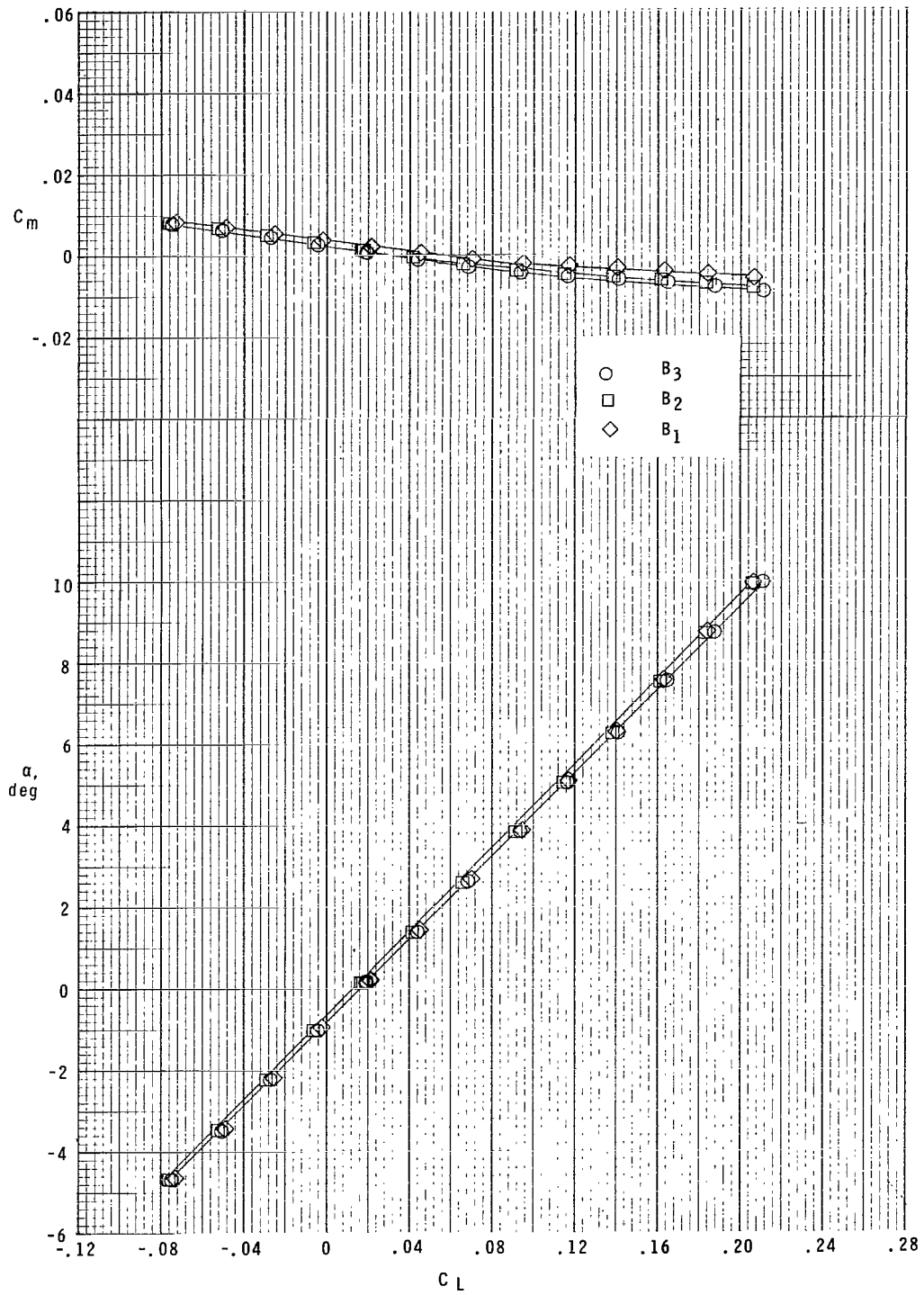
(b) $M = 3.25$.

Figure 5.- Continued.



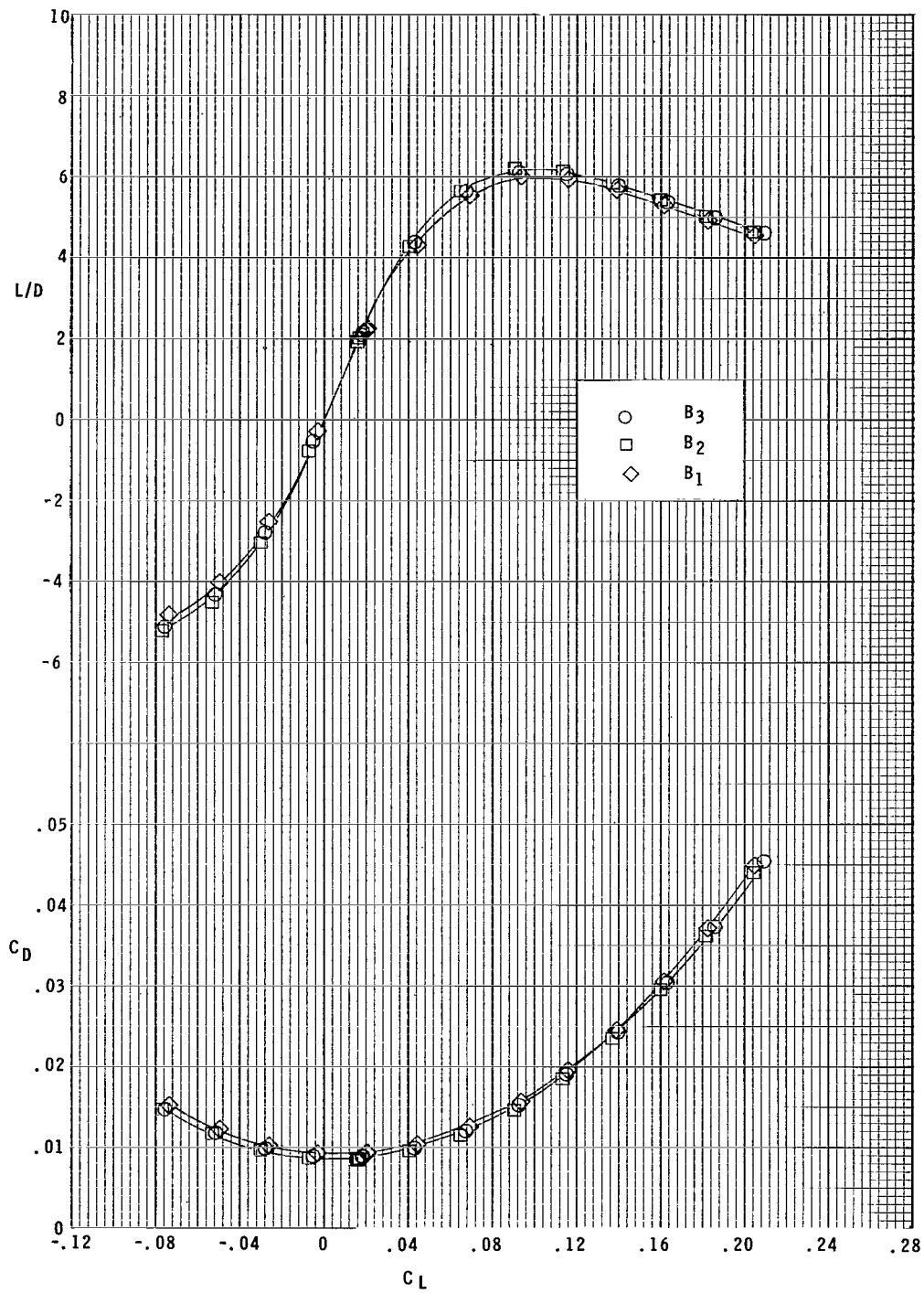
(c) Concluded.

Figure 5.- Continued.



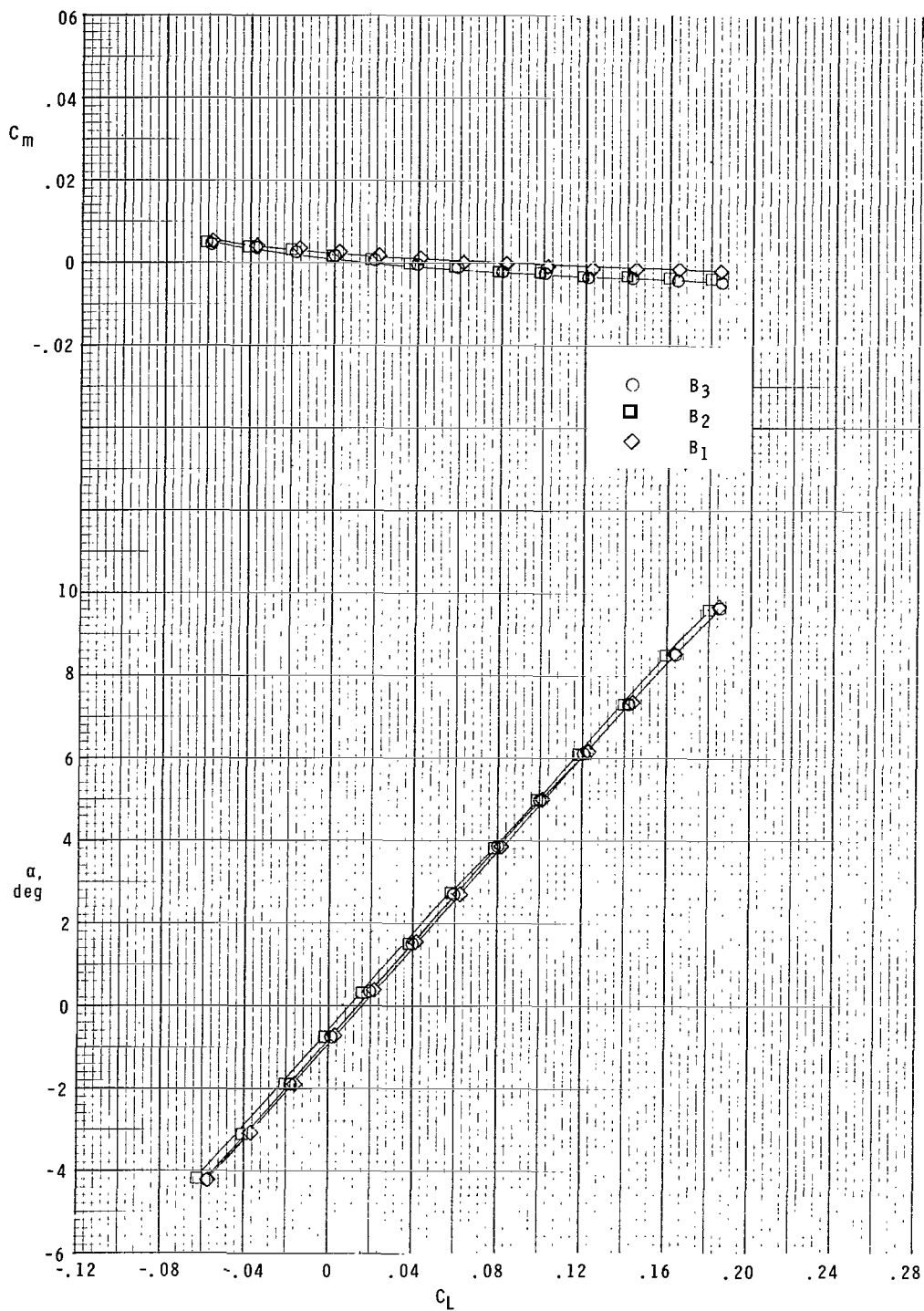
(d) $M = 4.00$.

Figure 5.- Continued.



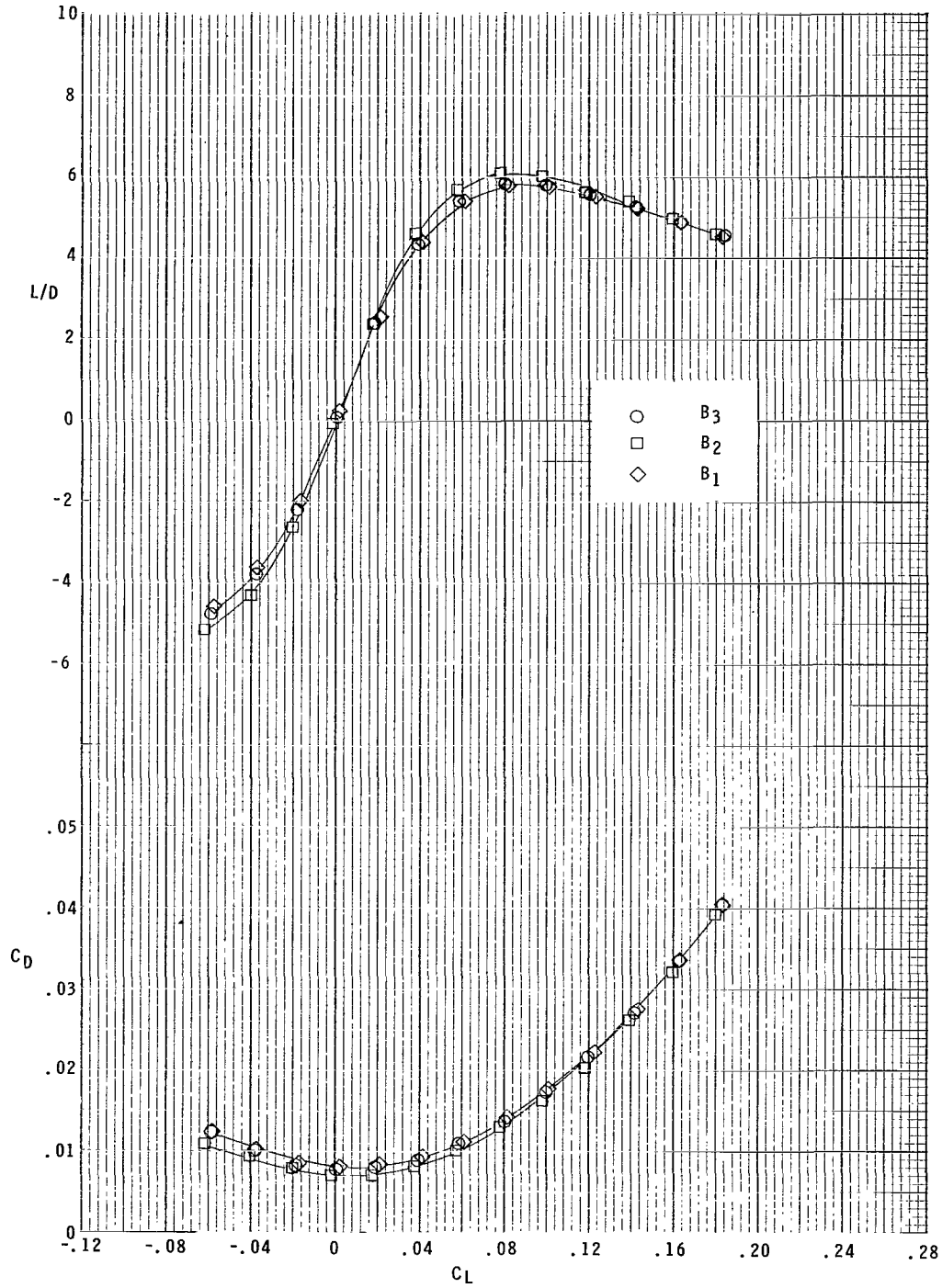
(d) Concluded.

Figure 5.- Continued.



(e) $M = 4.63$.

Figure 5.- Continued.



(e) Concluded.

Figure 5.- Concluded.

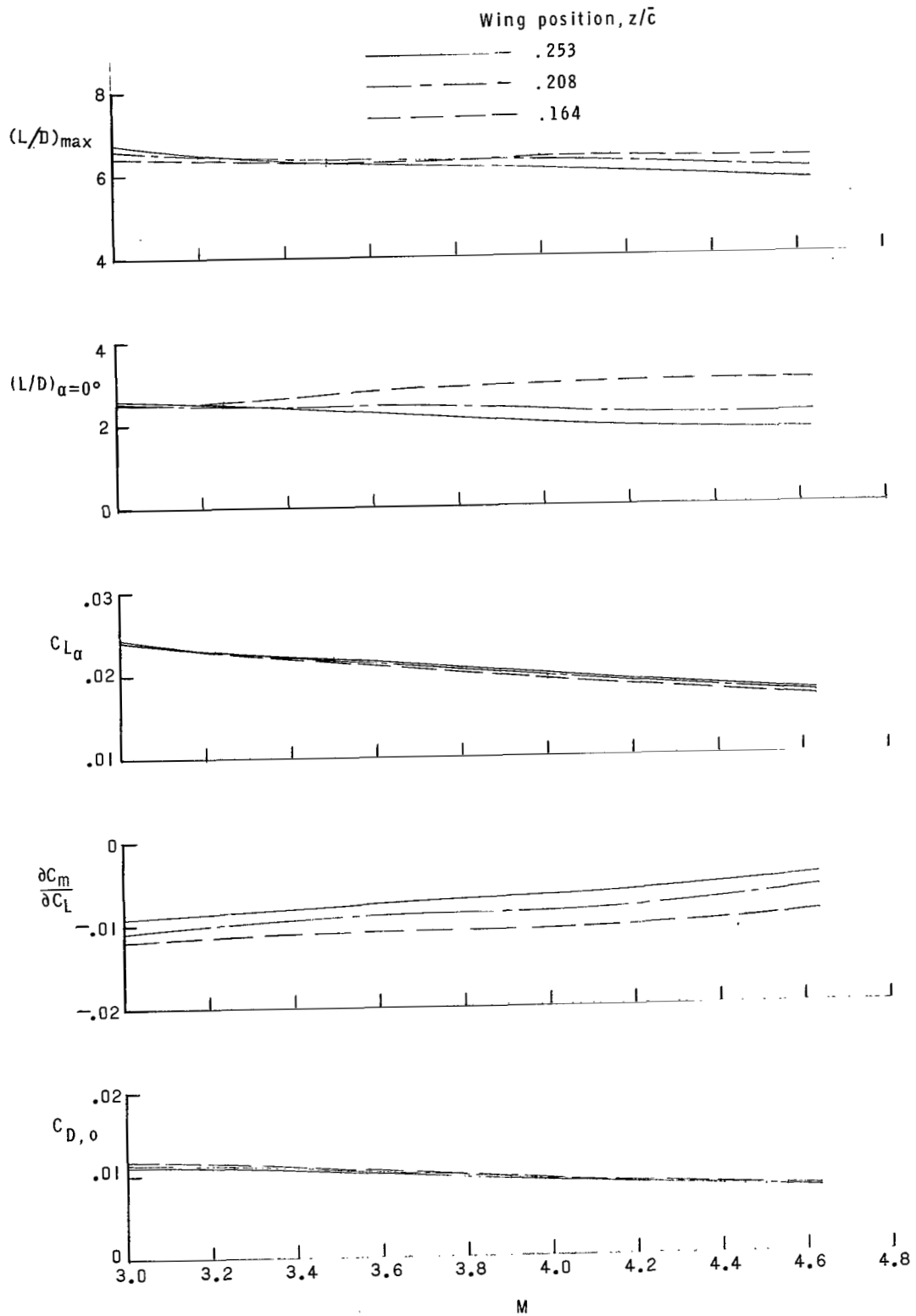


Figure 6.- Variation of the longitudinal parameters with Mach number for body 3 with three vertical wing positions.

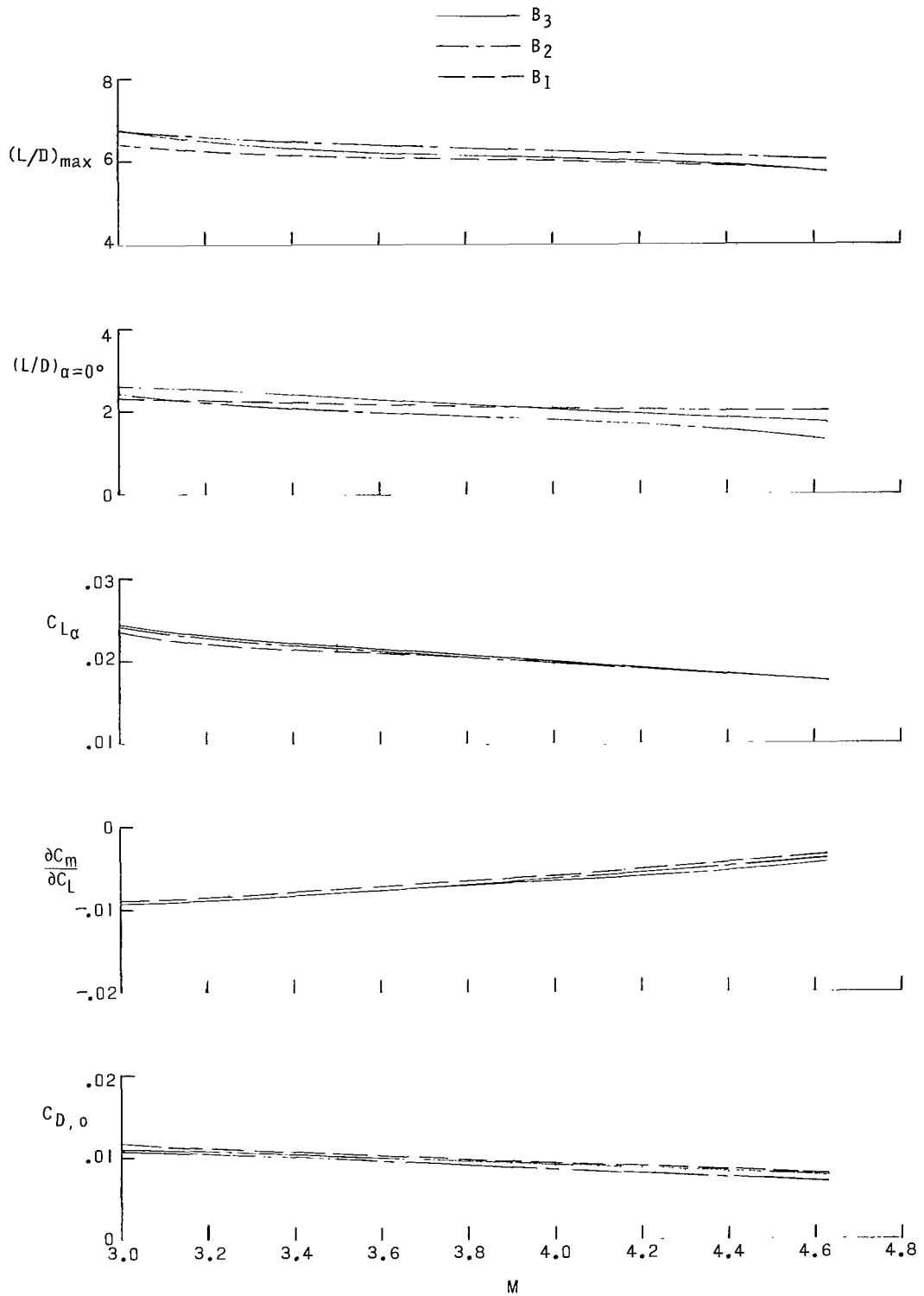


Figure 7.- Variation of the longitudinal parameters with Mach number for the three body shapes with the high wing position.

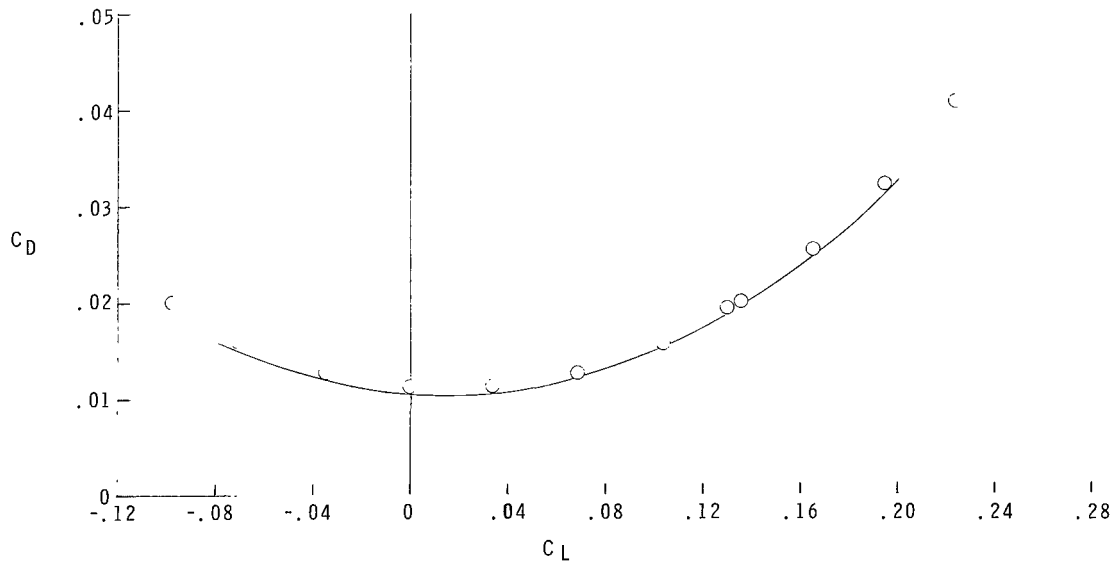
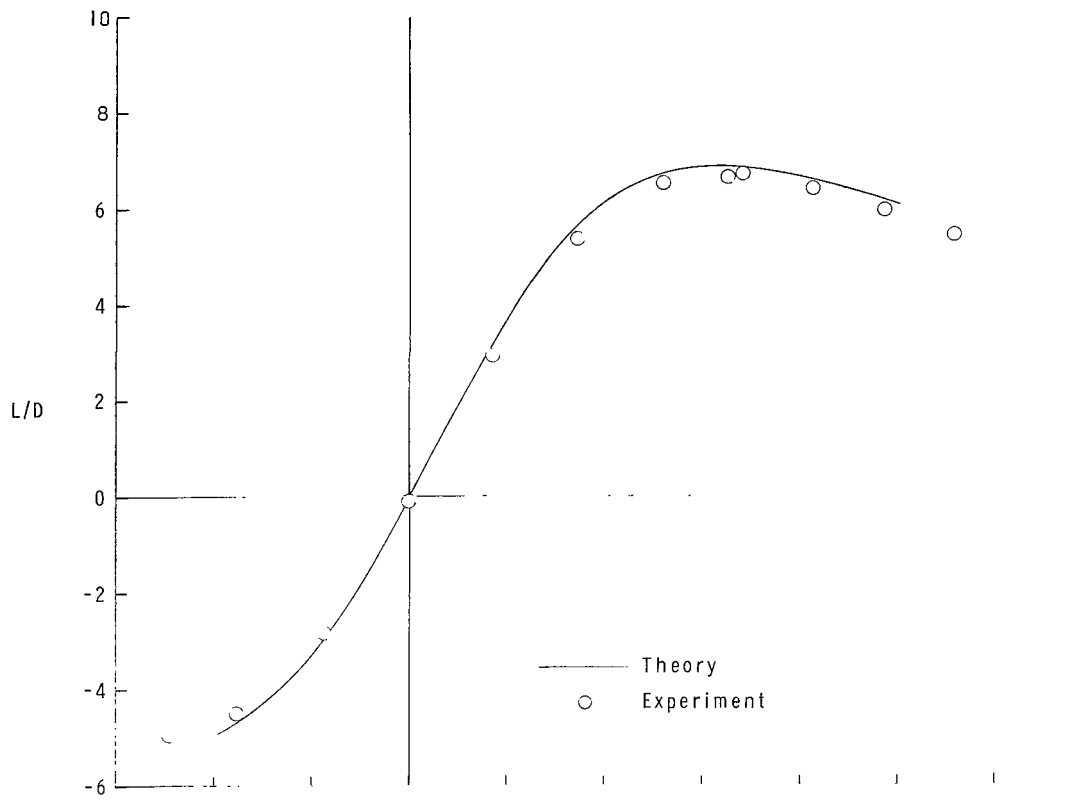


Figure 8.- Theoretical and experimental lift and drag results for the basic body with the wing in the high position. $M = 3.00$.

FIRST CLASS MAIL

05U 001 26 51 3DS 68285 00903
AIR FORCE WEAPONS LABORATORY/AFWL/
KIRTLAND AIR FORCE BASE, NEW MEXICO 87117

ATTN: E. LOU BOWMAN, ACTING CHIEF TECH. LIAISON

POSTMASTER: If Undeliverable (Section 158
Postal Manual) Do Not Return

"The aeronautical and space activities of the United States shall be conducted so as to contribute . . . to the expansion of human knowledge of phenomena in the atmosphere and space. The Administration shall provide for the widest practicable and appropriate dissemination of information concerning its activities and the results thereof."

— NATIONAL AERONAUTICS AND SPACE ACT OF 1958

NASA SCIENTIFIC AND TECHNICAL PUBLICATIONS

TECHNICAL REPORTS: Scientific and technical information considered important, complete, and a lasting contribution to existing knowledge.

TECHNICAL NOTES: Information less broad in scope but nevertheless of importance as a contribution to existing knowledge.

TECHNICAL MEMORANDUMS: Information receiving limited distribution because of preliminary data, security classification, or other reasons.

CONTRACTOR REPORTS: Scientific and technical information generated under a NASA contract or grant and considered an important contribution to existing knowledge.

TECHNICAL TRANSLATIONS: Information published in a foreign language considered to merit NASA distribution in English.

SPECIAL PUBLICATIONS: Information derived from or of value to NASA activities. Publications include conference proceedings, monographs, data compilations, handbooks, sourcebooks, and special bibliographies.

TECHNOLOGY UTILIZATION PUBLICATIONS: Information on technology used by NASA that may be of particular interest in commercial and other non-aerospace applications. Publications include Tech Briefs, Technology Utilization Reports and Notes, and Technology Surveys.

Details on the availability of these publications may be obtained from:

SCIENTIFIC AND TECHNICAL INFORMATION DIVISION
NATIONAL AERONAUTICS AND SPACE ADMINISTRATION
Washington, D.C. 20546